Organic Geochemical Study of Permian Series from the Jeffara and Dahar areas (Southern Tunisia) : Identification and Characterization of a Tunisian Permian Source Rock

Khawla Ouirghi, Amina Mabrouk El Asmi, Anis Bel Haj Mohamed, Moncef Saidi, Maria-Fernanda Romero-Sarmiento

Organic geochemical study of Permian series from the Jeffara and Dahar areas (Southern Tunisia): Identification and characterization of a Tunisian Permian source rock

Khawla Ouirghi[1,*] khawla.ouirghi@fst.utm.tn**, Amina Mabrouk El Asmi[1], Anis Bel Haj Mohamed[2], Moncef Saidi[2], Maria-Fernanda Romero-Sarmiento[3]**

[1]*Geology Department, Faculty of Sciences of Tunis, University of Tunis El Manar, 2092 Tunis, Tunisia*.
[2]*Entreprise Tunisienne des Activités pétrolières, 4 rue des Entrepreneurs, Charguia II, 2035*
[3]*IFP Énergies nouvelles (IFPEN), Direction Sciences de la Terre et Technologies de l'Environnement, 1 et 4 avenue de Bois-Préau, 92852Rueil-Malmaison Cedex, France*.
[*]Corresponding author.

ABSTRACT

Permian rock samples from four wells drilled in the Jeffara (J1 and J2) and Dahar (D1 and D2) areas of southern Tunisia were evaluated using the Rock-Eval® Shale Play™ method. Quantification of most liquid hydrocarbon compound families released at specific temperature range for the Sh0 and Sh1 as well as Sh2 and S3 parameters was achieved with subsequent calculations of appropriate indices. In addition, stable carbon isotopes evaluation of Permian samples was carried out in order to estimate the origin of their fossilized organic matter. Biomarker analyses were also undertaken on Permian samples and other proven Paleozoic source rocks samples of the study area (Ordovician Azzel and Upper Silurian Fegaguira formations) for comparison purposes.

The results show that the Permian series encompass highly-rich organic matter intervals which may exceed 5%. The organic matter is of type II2-III, proven either by the Rock-Eval®, carbon isotopes and biomarker data. Permian samples from three wells (D1, D2, and J2) are found mostly at an early mature stage. Contrary, Permian samples from the J1 Well show abnormal T_{max} temperatures testifying an overmature stage which could be related to abnormal heat flow around the Jeffara area. The depositional environment of the organic matter-rich Permian intervals is mainly suboxic of normal salinity, similar to the other Paleozoic investigated source rocks in the study area. Overall, this research comes to validate

the occurrence within the Dahar and Jeffara areas of an active Permian oil/gas prone source rock, competitive to the other proven Paleozoic source rocks.

Keywords

Permian, Southern Tunisia, Rock-Eval® Shale Play™ method, stable carbon isotope, biomarker, source rock.

1. Introduction

In Tunisia, the subsurface Paleozoic series have been targeted, for decades long, for petroleum exploration and exploitation, either for source rock or for reservoir rocks characterization and identification. Ordovician, Silurian and Devonian series, as well as the Mesozoic Triassic series have been scrutinized in order to identify prolific petroleum systems in southern Tunisia (Mejri al., 2006); however, Permian series were frequently underestimated and were the least inspected.

Furthermore, previous geological and geochemical studies have mostly focused on three main stratigraphic levels, the Silurian Tannezuft and Fegaguira formations and the Devonian Aouinet Ouenine Formation, considered fairly to highly-rich in organic matter (OM) and measured as pivotal potential source rocks of hydrocarbons in the region (e.g. Underdown and Redfern, 2008.); nevertheless, these source rock have a limited geographic distribution (Ben Ferjani et al, 1990). Consequently, more interest is currently given to other geological horizons such as the Middle Ordovician Azzel Formation or the Permian series, long overlooked, to identify potential functioning petroleum systems. Within this context, Permian series are suspected to bear significant petroleum potential. Indeed, and in some boreholes of southern Tunisia where Permian series were encountered, total organic carbon

(TOC) contents may reach 2.7% with a residual oil potential varying between 0.8 and 5.5 kg / ton of rock (Duvernoy, 1994).

The Permian series were also previously studied by various authors from a sedimentological, petrophysical and petroleum point of view since early thirties (Berkaloff, 1932; Douvillé et al.1933; Solignac; Berkaloff, 1933 and Douvillé,1934; Matthiew, 1949; Termier,1955, 1957, 1958, 1974; Termier et al, 1977; Glintzboeckel; Rabaté,1964 and Baird,1967; Newell et al.,1976; Razgallah and Vechard,1986; Chaouachi et al.,1987; MRabet et al.,1987; Chaouchi, 1988; Razgallah et al.,1989; Duvernoy and H 'Midi, 1994; Bouaziz , 1995). It is worth noting that Paleozoic series do not outcrop in Tunisia and are overall crossed through boreholes, except for the Permian series, which besides being encountered in subsurface, do also outcrop in Jebel Tebaga of southern Tunisia (Governorate of Medenine; Chaouachi, 1988). This outcrop constitutes the unique Paleozoic land-section of the entire country. However, in the Ghadames Basin and in the Chotts area of southern Tunisia, Permian series are exclusively encountered in boreholes. Furthermore, and according to borehole reports provided by ETAP (Entreprise Tunisienne d'Activités Pétrolière), the Permian series include frequent oil shows and dark black intervals which may include high amounts of organic matter.

On another level, classical organic geochemical techniques are widely used to characterize shale oil and gas play systems (e.gs, Espitalié et al., 1977; Espitalié et al., 1985; Lafargue et al., 1998; Jarvie, 2012; Song et al., 2017; Romero-Sarmiento et al., 2017). More recently, this technology has been also applied to characterize organic matter in recently discovered sediments (younger than 120ky) (e.g., Baudin et al., 2015) and soils (e.g. Soucémarianadin et al., 2018). Futhermore, a characterization program for unconventional shale resource systems was developed by IFPEN (France): the Rock-Eval® Shale Play method™ (Romero-Sarmiento et al., 2014, 2016; Pillot et al., 2014), allowing a better estimate quantification of

hydrocarbons (peaks Sh0 and Sh1) and a more precise determination of the thermal maturity parameter (T_{max}). Nonetheless and despite the overall reliability of the technique, the organic matter type and its origin, the mineralogy and the grain types of the hosting rock may sometimes bias the Rock Eval released parameters (Hunt, 1991; Spiro, 1991; Vu et al., 2013; Hazra et al., 2017; Carvajal; Ortiz & Gentzis, 2018; Abarghani et al., 2019; Hazra et al., 2019; Scheeder et al., 2020; Yang and Horsfield, 2020; Hazra et al., 2021; Karayigit et al., 2021). Data checking and the confrontation with results obtained for example from organic matter petrography, GC/MS analyses on source rocks extracts or from carbon isotopic results, can readjust such uncertainties.

Stable carbon isotope ($\delta^{13}C$) analysis is one of the useful indices used to determine the types of organic matter in source rocks (Pancost et al., 1999; Qu et al., 2019). The organic isotopic values of kerogen are controlled by the types of source organic matter. For instance, the values of carbon isotopes of the advanced land plants are generally relative to lower aquatic plankton (Whiticar 1996; Mccarren et al. 2008). Therefore, the carbon isotopic values of kerogen can be used to distinguish the different types of organic matter from source rocks.

Added to these techniques, the analysis of biomarkers by gas chromatography coupled with mass spectrometry (GC-MS) is of great significance in the determination of origin and maturity of organic matter. These biomarkers exist within a complex mixture of organic matter recording all the stages of accumulation, preservation and hydrocarbons migration. In addition, they are "*molecular fingerprints*" capable of highlighting the entire chemical or biological assessment processes and provide information about depositional environments (e.g. Peters & Moldowan, 1993; Peters, et al., 2005; Waples & Curiale, 1999; Cesar and Grice 2018; Luo et al. 2019).

Based on all the above, and aiming to evaluate the Permian series petroleum potentiality, the work herein presents a geochemical study of dark layers encompassed within the Permian series in four drilled boreholes located in the Jeffara Basin and Dahar areas of Southern Tunisia (Fig.1). This is focal as, up to date, no previous geochemical studies have been published on the Permian petroleum potential of southern Tunisia except of internal reports or oral communications. The present study uses specific organic geochemical techniques for the evaluation and characterization of source rocks. More specifically, the study assesses the organic matter present in Permian intervals trying to evaluate its richness, nature, thermal maturity, depositional environment, through the use of a combination of several analytical techniques: Rock-Eval® Shale Play™, the GC-MS technique (biomarkers) and stable carbon isotopes analyses in order to estimate potentially producible oil intervals.

2. Geological setting

The study area is the Northern edge of the Saharan platform (Fig.1). It is limited to the northeast by the central Mediterranean Sea, to the Northwest by the Chotts area, and to the south by the Tunisian-Libyan border. From a geological point of view, the Saharan platform remained stable since the late Paleozoic, but to the north, a strong subsidence created the Jeffara basin (Fig.1). After the Carboniferous-Permian Hercynian phase, a generalized NE-SW Permian extension took place splitting the Pangea (Arthaud and Matte, 1977), together with the Eurasian/African dextral sliding, responsible for the opening of the Neotethys (Bouaziz et al., 1999). This extensive movement led to the compartmentalization of the Jeffara into horsts, grabens and tilted blocks, delimited by EW major faults separating a carbonate platform in the South from a subsiding basin in the north (Raba,1988; Ben Ferjeni et al.,1990 et Mejri et al., 2006). It was followed by a significant subsidence leading to marine Permian deposits in the Tebaga basin (Touati and Rodgers, 1998) with thicknesses reaching 3000 m. This extensive regime continued until the middle Triassic allowing the final shaping

of the Jeffara basin (Busson, 1967; Newell et al., 1976; Khessibi, 1985; Ben Ayed, 1986; Toomey, 1991; Bouaziz, 1986, 1995). The Hercynian orogeny led to a major regional erosion of hundreds of meters of Carboniferous and early Permian sediments (Bouaziz, 1995). This was followed by Mesozoic subsidence changing to tectonic inversion with prevailing compressional movements of the Alpine orogeny during the Cenozoic (Bouaziz et al., 1999). Although the Saharan platform remained stable since the Late Paleozoic, the Permian basin was crossed by a major shear fault system (Ben Ayed, 1986; Bouaziz, 1986; M'rabet et al., 1987) corresponding to the Gafsa-Jeffara fault zone that extends from the southern Atlas in the northwest to the Nefusa uplift in the southeast (Ben Ayed, 1986; Ben Hassan et al., 2014; Bouaziz, 1986; M'rabet et al., 1987) (Fig. 2). Of note, the only outcropping Permian marine sediments of North Africa occurs within this fault zone at the Jebel Tebaga near Medenine (Newell et al., 1976; Driggs, 1977; Toomey, 1991). Overall, the Permian series could only be recognized by cores of exploration wells (Ben Ismail, 1991; Bouaziz, 1995) and outcrop (Chaouachi, 1988; Ben Ismail, 1991; Bouaziz, 1995) occur uniquely to the North of the Telemzane Arch (Fig. 2). Therefore, the study area is located within this domain which shows various facies ranging from siliciclastic shallow deposits, reefal constructions to deeper marine carbonate deposits (Zaafouri et al., 2017).

3. Material and methods

3.1 Sampling

74 investigated rock samples derive from four exploration wells, two drilled in the Jeffara basin (J1 and J2; Figs 1,3) and two of them in the Dahar area (D1 and D2; Figs 1, 3). The studied Samples, which are mainly shaly carbonates in facies, were chosen within the Permian series on the basis of their richness in organic matter and their blackest color. Sample's selection was performed as follow (Table 1):

- Nine samples from the D1 Well ;

- Nineteen samples from the D2 Well;
- Sixteen samples from the J1 Well;
- Thirty samples from the J2 Well.

In addition, five cuttings samples were selected for GC/MS analyses (Table 2): Three cuttings samples from the Permian series of the D1 and D2 wells and two other samples from known source rock of the area, one from the Silurian Fegaguira source rock and one from the Ordovician Azzel source rock (Table 2). It is worth clarifying that the choice of only three samples from the studied wells was based on their richness in TOC and their free hydrocarbon issued by the Rock Eval pyrolysis. They were considered as representative of all studied Permian samples to be scrutinized from a biomarker point of view. The other two samples (Ordovician and Silurian) were selected for organic matter biomarkers comparison with the organic matter biomarkers of the studied Permian samples.

Carefully grinded and powdered samples to around 63 μm, were used for Rock-Eval® Shale Play™, stable carbon isotopes and biomarkers analyses.

3.2 Rock-Eval® Shale Play™ method

The crushed samples were first characterized by open-system pyrolysis using a Rock-Eval® 6 (e.g., Espitalié et al., 1985; Lafargue et al., 1998; Behar et al., 2001) device operated at IFP Energies nouvelles (IFPEN - France). This technique was used here to determine the Rock-Eval® Shale Play™ parameters (e.g. Sh0, Sh1, HC content, HQI, PIShale) as well as a more accurate thermal maturity of the investigated samples. This method was also used to estimate the TOC content and the kerogen type of the selected rock samples, the source rock quality and the thermal maturity of organic matter. For these purposes, the Rock-Eval® Shale Play™ method was tested on 40 mg of powdered samples following the procedure described in Romero-Sarmiento et al. (2015; 2016; 2017). The Rock-Eval® Shale Play™ method is characterized by a starting thermal vaporization step at low temperature (100°C). Then, the

oven temperature increases from 100°C to 200°C, and following this rise, it is raised again from 200°C to 350°C and finally the pyrolysis temperature increases from 350°C to 650°C at 25°C/min. Two plateaus of 3 minutes are imposed at 200 and 350°C (Romero-Sarmiento et al. 2014; 2016 a,b). The quantity of hydrocarbon compounds released during the thermal vaporization step from 100°C to 200°C corresponds to the Sh0 parameter. The Sh1 parameter provides the quantity of hydrocarbon compounds released during the thermal vaporization step from 200°C to 350°C and the Sh2 parameter provides the quantity of hydrocarbon compounds released during the final pyrolysis step from 350°C to 650°C (Romero-Sarmiento et al. 2014; 2016a,b).

3.3 Decarbonation

Based on Rock-Eval® Shale Play™ results, a total of twenty samples were selected (5 per well) to obtain the corresponding isolated OM (OM concentrate). These 20 samples do not include the five samples which were analyzed by GC/MS. The mineral matrix of the bulk rock sample is destroyed using non-oxidant acid (HCl) to remove carbonates, sulphides, sulphates, clay minerals, quartz and silicates. It is widely known that certain minerals remain after acid attacks, in particular pyrite. Finally, the obtained OM concentrates were analyzed by Rock-Eval® Shale Play™ to estimate the hydrocarbon content index of the OM concentrates (HCcont (OM) = Sh0 (OM) + Sh1 (OM), in milligrams of HC per gram of OM concentrate.

3.4 Stable carbon isotope analysis

In this study, stable carbon isotope ($\delta^{13}C$) analyses were only performed on 20 isolated organic matter concentrates, as five rock samples showing high TOC values were selected for each investigated well (four samples per well), and obtained by destroying the carbonate matrix with HCl acid treatment.. The stable carbon isotope analyses were carried out using a ThermoFischer Scientific EA - Isolink II-MAT253 spectrometer operated at IFPEN (France).

The stable carbon isotope data are presented in the δ notation relative to V-PDB standard with the analytical precision estimated to be ± 0.2 ‰.

3.5 Biomarkers

A total of selected five Permian cuttings samples were analyzed in this study, for GC-MS analysis, in which three of them are from the D1 and D2 wells and two from known source rocks of the area (Fegaguira and Azel formations)

The organic extraction was carried out by a Soxhlet apparatus using dichloromethane. Afterwards, the solvent was removed by means of a rotary evaporator. The extracts were separated into their saturated fractions employing the standard mini-column chromatography (e.g., Behar et al, 1984). The saturate and aromatic biomarkers were determined using Agilent 7890A gas chromatograph coupled to an Agilent 5973 Series Mass Selective Detector (Peters et al., 2005). The separation was carried out using a DB-1MS fused silica capillary column of 30m length, 0.25mm inner diameter and 0.25μm film thickness. Helium was used as a carrier gas with a flow rate of 1 ml/min. The oven temperature used to analyse saturates was programmed from 50°C (2 min) to 170°C at 5°C/min and to 300°C at 1.5°C/min. The ion source was operated in electronic impact (EI) mode at 70 eV at 280°C. The MS was operated in selective ion monitoring (SIM) for the following ions: alkanes (m/z 57), steranes (m/z 217), and terpanes (m/z 191). Biomarker identification was performed using published data and laboratory records.

4. Results and Discussion

4.1 Source rock quality, organic matter type and thermal maturity

Free and sorbed liquid hydrocarbons (Sh0 and Sh1 peaks), that could be present in studied samples (e.g., Romero-Sarmiento et al., 2015; 2016; Fig.4; Table1), were quantified using the Rock-Eval® Shale Play™ method.

Figure 5 shows free and/or sorbed liquid hydrocarbon content (HCcont = Sh0 + Sh1; Table 1) versus TOC content. A positive correlation between the total quantity of hydrocarbons (Sh0 + Sh1 in mg HC / g of rock) and TOC values is observed for Permian samples of the different wells. However, most of the studied samples show low to medium oil saturation, the oil crossing the effect and potential productive intervals were identified in three samples from well J2 (samples J2-S_{21}, J2-S_{23} and J2-S_{24}). Sample J2-S_{26} shows also good oil potential. The Permian specimen of the J1 Well (Table 1); however, reveal relatively low TOC contents, which rarely exceed 0.50%, recorded in the majority of samples. Nevertheless, intervals preserved high amounts of organic matter with TOC contents that can reach up to 7.76% in well D1 (Table 1, Fig.6), 7.69 in J2 (Table 1, Fig.7), 1.32% in J1 (Table 1, Fig.8) and 5.54% in D2 (Table1, Fig.9).

Overall, the Permian series are generally rich in organic matter (OM) and the obtained TOC values varied between 0.5% and 7.76% with an average of 4.13 % (Table 1). The results demonstrate that the J1 samples are characterized by low residual oil potentials that did not exceed 0.40% mg HC/g.rock due to either to a very advanced thermal maturity or a poor quality of the oil. The organic matter could have been poorly preserved during its deposition (Hunt, 1996; Vecoli, et al., 2009). Conversely, the other wells D1, D2 and J2 have a high oil potential that can reach 31.46 mg HC/g rock, for the well D1, 21.08 mg HC/g rock, for D2, and 12.69 mg HC/g rock for J2.

The HI (HI = Sh2 100/TOC) / TOC and (SH2/S3) /TOC diagram (Fig. 10 and Table 1) is classically used to provide information on the type of generated hydrocarbon (Espitalié et

al., 1986) by the analyzed rocks. The diagram presented in the Fig. 11 reveals that the source rocks of J2 and D2 generated an average quantity of oil.

T_{max} is a widely used parameter for evaluating the thermal maturity (Espitalié et al., 1977), but may also be influenced by kerogen type (Hunt, 1996; Vecoli, et al., 2009, Vu et al., 2013, Yang and Horsfeld, 2020 and Karayigit et al. 2021). Indeed, the Hydrogen Index (HI) and/or the Oxygen Index (OI) when correlated to T_{max} (HI = Sh2 *100 / TOC) / T_{max} (Sh2 peak maximum temperature; Fig. 10 and Table 1) may possibly imply the organic matter origin in the analyzed samples (Espitalié et al., 1986). Based on thermal maturity, the T_{max} (Sh2 peak maximum temperature) Rock-Eval® Shale PlayTM values, recorded in the Permian age samples taken from Well D1, depending on depth and oscillate from 435 to 439 ° C in the interval (2144 -2393m), corresponding to the early stage of the oil window.

The values of T_{max} recorded at the lower parts of D2 and J2 wells ranged from 431°C to 450°C, and these samples are early mature to mature. On the other hand, the studied samples from J1 display very high values which are exceeding 500 °C, demonstrating an over-mature organic matter. This can be explained by the NW-SE crustal lithospheric anomaly, which could have caused a high mantle heat flux located within the Jeffara basin (Gabtni, 2006). A crustal thinning would have created a significant burial of sedimentary layers associated to the manifested rifting (McKenzie 1978; Wernicke, 1981; Barbier et al., 1986; Doglioni, 1994 in Gaptni., 2006). This burial started during the Late Carboniferous and may have lasted up to the early Permian (Memmi et al., 1986 in Gaptni., 2006; Fig. 12). This was confirmed through the variation of geothermal flux, identified in the region compared to the average geothermal gradient. In fact, the distribution of the geothermal flux in terms of "heat-flow density" (HFD) at the level of the Mediterranean basin and, in particular, at the southern segment of the Geotraverse (EGT-S) campaign, shows a heat flux anomaly superior than 100 MW/m^2 in the Jeffara region (Bouaziz et al., 2015; Gabtni., 2006; Mraidi et al.; 2021; Fig. 12 (C)).

The analyzed samples show relatively low values of HI in all studied wells (D1, D2, J1, and J2) varying between 18 and 300 mg HC / g TOC, typical of mixed organic matter between type III of continental origin and type II of marine planktonic origin. The HI/OI diagrams (Fig.13 (A)), HI / T_{max} (Fig. 11) and Sh2 / TOC (Fig.13 (B)) made it possible to determine the type of organic matter (Hunt, 1996; Vecoli, et al., 2009) in the different studied samples (Fig. 13 A-B). The location of the representative points of the analyzed samples on the HI/OI and HI/T_{max} diagram indicates that their organic matter is of mixed origin between terrestrial origin and marine origin, especially for samples from D1, D2, and J2 W well. We may note, that the poor preservation of Permian organic matter in the J1 well may have resulted in its oxidation, hence its leaning to the type III-IV organic matter as presented in the diagram (Fig. 13).

4.2. Bulk carbon isotope interpretations

After de-carbonation, TOC contents, as expected, became very high reaching a maximum equal to 15.26% for the de-carbonated sample J-S26, while the Minc % percentages became very low of the order of 0.61 against 9.14 for the sample D1-S4, which shows that the de-carbonation process was effectively carried out (Fig. 14 ; Table 3).

Figure 14 illustrates the bulk carbon isotope ($\delta^{13}C$) results obtained from investigated samples. The stable carbon isotope signature was determined to establish the type of OM present in source rocks and the relationship of this OM with the depositional environment (Meyers, 1994; Calvert et al., 1996). Indeed, the organic carbon isotope (δ13Corg) contents of the source rocks are presented below:

For the D1 well, the δ13Corg values were -22.65 ‰, -18.95 ‰, -25.21 ‰, -24.01 ‰ and -23.90 ‰, with an average value of -22.9 ‰. For the D2 well, they were -19.18 ‰, -21.45 ‰, -21.80 ‰, -20.72 ‰ and -21.36 ‰, with an average value of 20.9 ‰. For well J1, these values were -22.12 ‰, -23.69 ‰, -21.95 ‰, -24.23 ‰ and -24.53, with an average value

equal to -23.3 ‰. For well J2, they reached -21.83 ‰ -23.72 ‰, -23.24 ‰, -26.28 ‰ and -22.62 ‰, with an average value of -23.5 ‰.

The δ13C contents of studied Permian samples reflects no major difference among the studied wells. Furthermore, this data can be efficiently used for the determination of the types of OM in source rocks (Pancost et al. 1999). The OMs in the sedimentary rocks are generally classified into three types according to the difference in the micro-components of kerogen defined as insoluble organic matter: type (I), type (II) and type (III), (Straussand Peters-Kottig, 2003; Thomas et al., 2004; Hermann et al., 2010). Besides, the δ13C isotope content of kerogen remains the same as that of the organism source material (Forsman and Hunt 1958). The δ13C isotopic values of kerogen are controlled by the types of parent OM (Whiticar 1996; Mccarren et al. 2008). Therefore, kerogen δ13C isotopic values can be employed to distinguish organic material types from source rocks (Grasby and Beauchamp, 2008; Luo et al., 2014). The division of kerogen types of organic matter according to carbon isotope ratio values (Meyers, 1997) is presented in Figs 15-17.

Previous studies indicated that the δ13C isotope values of terrestrial plants are generally equal to -21.60 and -26.70 ‰, while the δ13C isotopic values of aquatic plankton vary between -27.60 and -32.60 ‰, (Ehleringer 1991; Angradi 1994; Qin 2005; Yang et al. 2014). In this study, the δ13C isotopic values of Permian age source rocks extracted from the different wells are in the kerogen range of type II2 / III (Table 3). The δ13C isotopes values coupled to the Rock-Eval® Shale Play™ results confirms a terrestrial origin of organic matter deposited in a marine setting.

The comparison of the %C after elemental analysis and TOC obtained by the Rock-Eval® Shale Play™ analysis after de-carbonation shows a strong correlation between % C and the TOC (Fig. 18) which is confirmed by the recorded quantity of TOC available in each sample (Fig. 19). In order to demonstrate that the values of δ^{13}Corg do not respond

exclusively to the amount of organic carbon present in the sample, we describe the relationship between δ^{13}Corg and TOC (Fig. 19), the calculated R^2 value for their relation is (R^2 = 0.1729 for J1; R^2 = 0.1321 for D2; R^2 = 0.3995 for D1; and R^2 = 0.4162 for J2), which highlights the fact that δ13Corg is not dependent on the TOC (Hartke et al., 2021).

4.3 Source-rock hydrocarbon potential from Tunisian Permian series

Based on Rock-Eval® pyrolysis results, some analyzed intervals of the Permian series in the different studied wells hold a moderate source rock potential. Indeed, the interval 1549m - 2282m (Fig.6) for the D1 well, the interval 986m - 1560m (Fig. 7) for the D2 well and the interval 1175 – 1296 (Fig. 8) for the J2 well are moderately rich in organic matter of "Oil- and Gas- prone" quality and which can be retained as petroleum source rocks. The common kerogen type in these samples is type II/III, of terrestrial origin, which was transported into marine setting; however, the analyzed Permian series of the J1 Well (Fig. 9) are lacking any source rock potential coupled to the fact that samples are over-mature, probably due to an anomaly in the heat flow in the region.

4.4. *Biomarker distributions and palaeoenvironmental conditions*

4.4.1 Alkanes fingerprinting

Saturated hydrocarbons chromatograms of the Azzel and Fegaguira samples show slightly developed UCM (Unresolved Complex Mixture), testifying that the extracts were partially biodegraded (Gough and Al., 1990). The total ion chromatogram (TIC) represents the distribution of *n*-alkanes and *iso*-alkanes. Based on Eglinton and Hamilton, 1967; Meyers, 1997; Tissot and Welte, 1984; Peters et al., 2005; the abundance of short-chain *n*-alkanes indicates an algal derived organic matter. Nonetheless, The TIC of the saturated hydrocarbon fraction (Fig.20) displays a unimodal distribution of *n*alkanes going from *n*-C_{15} to *n*-C_{35} centered with low molecular weight (C_{17}) regular decrease beyond n-C17; therefore, a marine setting is inferred based on Blanchart, 2011 ; Hu et al., 2013.

Both source rock samples show in general a predominance of 2,6,10,14- tetramethyl hexadecane (phytane), compared to 2,6,10,14- tetramethyl pentadecane (pristane) (Fig. 20). Samples, D1-S4, D1-S5 and D2-S16, show a unimodal distribution of n-alkanes ranging from *n*-C_{13} to *n*-C_{34} and a UCM of low intensity (Fig.20).

Otherwise, these samples were characterized with a weak relation between Pr/*n*-C_{17} and Ph/*n*-C_{18} that did not exceed 0.53 and 0.73 (Fig.20; Table4).

4.4.2. Terpanes and Steranes

The mass fragmentograms *m/z*= 191 related to the distribution of terpanes of the studied samples show a predominance of tricyclic terpanes over pentacyclic terpanes (hopanes) in the Azzel and Fegaguira Paleozoic samples as shown by the high values of the C_{23}tr/H_{30} ratio (> 4) in contrast to the Permian sample (D1-S4, D1-S5 and D2-S16; Fig.21).

Pentacyclic hopanes are characterized by an abundance of 17α(H),21β(H)-trisnorhopane (H_{30}) compared to C_{29}-17α(H),21β(H)-trisnorhopane (H_{29}) indicating a clayey lithology of the studied rocks (Peters et al.,2005). A low concentration of Gammacerane was observed in all samples indicating that the organic matter was deposited and preserved in a marine environment of normal salinity (Venkatesan, 1989). The studied samples show low C_{35} homohopane/C_{34} homohopane (C_{35}/C_{34}H) ratios (<1) for Azzel, Fegaguira, D1-S4, D1-S5 and D2-S16, therefore indicating an oxic to suboxic depositional environment (Peters and Moldowan, 1993; Jiang and George, 2018).

The studied Azzel and Fegaguira samples show a predominance of 5α (H), 14α (H), 17α (H)-20R steranes (C_{27} steranes) compared to C_{28} and C_{29} steranes. The predominance of C_{27} steranes in these Ordovician (Azzel) and Silurian (Fegaguira) is indicative of an organic matter of marine origin (Volkman et al., 2003) that could have generated the free hydrocrabons (Fig.21). Conversely, the analyzed D1-S4, D1-S5, and D2-S16 Permian samples show an abundance of C_{27} and C_{29} compared to C_{28}. This abundance is significant of

a mixed organic matter of the type II/III (marine dominated with terrestrial organic matter input) which is responsible of the extracted free hydrocarbons.

4.4.4. Salinity

Gammaceranne is a C_{30} triterpane, a biomarker that plays an important role in discriminating the salinity of sedimentary water. (Jiafmo et al., 1986; Sinninghe Damsté et al., 1995). When samples show a low concentration of gammacerane, this reflects a normal salinity of their source rocks depositional environment. An abundance of gammacerane was well determined and associated with a hypersaline environment (Niu et al., 2018).

The gammacerane/hopane ratios of the different samples are low in the order of 0.05 for samples D1-S4, D1-S5, and D2-S16; and equal to 0.13 and 0.24 for Azzel and Fegaguira source rocks, respectively. Thus, it would appear that the depositional environment of the Azzel and Fegaguira source rocks is relatively more saline than that of the D1-S4, D1-S5 and D2-S16 samples.

4.4.5. Organic matter origin

Different parameters were used to analyze terpanes and steranes and provide information on the terrestrial or marine nature of the organic matter.

As demonstrated in the previous section, the variation of the C_{19} tricyclic terpane / (C_{19} tricyclic terpane + C_{23} tricyclic terpane) ratio as a function of C_{24} tetracyclic terpane /(C_{24} tetracyclic terpane+ C_{23} tricyclic terpane) (C_{19}tr / (C_{19}tr + C_{23}tr)) allowed differentiating the terrestrial origin from the marine origin of the OM in the Azzel, Fegaguira, and Permian source rocks (Table 4). The analyzed samples were characterized by very low to low C_{19}tr / (C_{19}tr + C_{23}tr) ratios and C_{24}Tet / (C_{24}Tet + C_{23}tr) ratios. These values did not exceed 0.19 and 0.10 for the Azzel and Fegaguira source rocks, respectively. They were moderately high for samples D2-S_{16} from (0.3) to high for samples (D1-S_4, D1-S_5) of the order of 0.4 and 0.5. The plotting of the representative points of the different analyzed samples, shown in the Fig. 22,

testifies the OM marine setting with a major terrestrial contribution in samples D1-S_4- D1-S_5, and D2-S16. On the other hand, D1-S_4 and D1-S_5 samples are also distinguished by relatively higher C_{24}Tet / C_{26}tr ratios (4.59), compared to the other two source rocks and D2-S16 sample, which confirms the input of terrestrial OM. Samples of the Azzel (Ordovician) and Fegaguira (Silurian) formations seem to be of almost exclusively marine origin. Overall, the ternary diagram (Fig. 22) confirms the previous result and indicates that the Azzel and Fegaguira source rocks were generated by essentially marine OM. The OM contained in Permian samples (D2-S16, D1-S_4, and D1-S_5) mainly has a terrestrial origin.

4.4.6. Redox condition

The ratios Pr / Ph, Pr / *n*C_{17} and Ph / *n*C_{18} were used to specify the nature of the depositional environment and to determine the lithology of source rocks (Peters and Moldowan, 1993; Peters et al., 2005). The studied samples are characterized by Pr / Ph ratios varying between 1.08 and 1.18 and by relatively low Pr / *n*C_{17} and Ph / *n*C_{18} ratios ranging between 0.33 - 0.50 and between 0.38 - 0,50, respectively. The plotting data of the examined samples on the Pr / *n*-C_{17} versus Ph / *n*-C_{18} diagram (Fig. 23) demonstrates that the OM in these samples was deposited in a dysoxic to anoxic environment.

The values of the C_{26} tricyclic / C_{25} tricyclic ratio and those of the C_{31}R (17α, 21 β (H)-homohopane (22R)) / C_{30} Hopanes ratio, in the Permian samples, indicate an essentially clay lithology of these rocks. The clay fraction was higher in the Azzel and Fegaguira source rocks than in the D2-S_{16}, D1-S_4 and D1-S_5 source rocks (Table 4). These hypotheses were confirmed by the position of representative samples points on the C_{27}βα 20R diasterane /C_{27}ββ 20S Steranes diagram as a function of C_{29}/C_{30} hopanes Homohopanes (Fig.24 (B)).

4.4.7. Maturity

The Ts / Tm ratio is often used to measure the degree of maturity (Peters and Moldowan, 1991).) with mature stage represented by a ratio higher than 1 (Ts / Tm> 1). The Azzel and

Fegaguira source rocks show high Ts / Tm values (> 1), while Permian samples (D2-S_{16}, D1-S_4 and D1-S_5) have a predominance of Tm over Ts (Ts / Tm <1), which testifies that they are in an early mature stage, unlike the other two samples. The location of samples on the $C_{27}\beta\alpha$ 20R diasterane /$C_{27}\beta\beta$ 20S Steranes versus 18α (H), 22, 29, 30-trisnorneohopane (Ts) / C_{27} 17*α*-22, 29, 30-trisnorhopane (Tm) diagram (Fig.25) confirms the difference in thermal maturity between the investigated samples. Fegaguira and Azzel samples showed ratios greater than 0.4, indicating that they are mature for hydrocarbon generation. Nevertheless, one Permian sample (D2-S16), appears to be the least mature compared to all analyzed samples with values of $C_{29}\alpha\alpha$S (5alpha, 14alpha, 17alpha, 24-ethylcholestane 20S)/C_{29}(S+R) and $C_{29}\beta\beta$ (5alpha, 14beta, 17beta, 24-ethylcholestane)/(αα+ββ) ratios below 0.4 (Fig.25).

5. Conclusions

Based on the Rock_Eval® Shale Play™ analyses results of analyzed samples from Permian series in the southern Tunusia, it is found that the Permian series encompass moderate to good source rock potential in three of the four studied wells (D1, D2, and J2). The OM of ¨Permian samples from these three wells is qualified as type II2 /III with a major terrestrial contribution, and seems to be in the early oil window stage. The identified OM in the Permian sediments of well J1 is oxidized in the depositional environment, and furthermore it has been affected by an abnormal heat testified by high T_{max} temperatures. This could be related to crustal thinning in the study area.

Carbon isotopes results (δ13C) concurs with some of the Rock-Eval® results and indicate that the organic matter within the Permian sediments is of type II2 / III.

High TOC selected Permian samples (D2-S16, D1-S_4, and D1-S_5) were subjected to further analyses via GC/MS analyses of their free oil extracts. All studied Paleozoic samples were found to belong to source rocks of marly-clayey lithology, in agreement with samples lithology. The OM deposition took place in a marine setting with relatively normal salinity,

and under dyoxic-anoxic conditions. The OM in the studied Permian series seems to have a mixed origin, and majority is derived from high terrestrial plant matter inputs into marine environment. Nonetheless, future palynological and palynofacies analyses should be undertaken in the future for better understanding of the OM origin in the studied Permian series.

The main outcome of this geochemical study is that it contributes to verify the petroleum potential of the Permian series of southern Tunisia as a moderate to good oil/gas prone source rock either in the Dahar or the Jeffara area. It is worth noting that studied samples herein belong to drilled wells on relatively high structures and laterally, where the Permian is more deeply buried, maturity could be more enhanced and hydrocarbon generation/expulsion could have occurred.

Lastly, further investigations combining geochemical results with geophysical interpretations and basin modeling are now needed to be able to achieve a volumetric assessment of the Permian source rock generated/expelled hydrocarbon amounts.

Acknowledgements

Authors greatly acknowledge the Entreprise Tunisienne d'Activités Pétrolières (ETAP) for providing necessary data and samples to accomplish the present study. They are also thanked for their help and support for GC/MS analyses. The IFP-Energies nouvelles (IFPEN - France) are deeply thanked for hosting the first author in their laboratories. Their analytical assistance and the realization of the Rock-Eval® Shale Play™ and stable carbon isotopes determinations helped to make this manuscript possible. The Tunisian Ministry of Higher Education is acknowledged for sponsoring the first author to achieve her training at the IFP-Energies nouvelles (IFPEN - France). Finally, we thank the editor and anonymous reviewers for constructive and helpful comments.

Declaration of interests

The authors declare that they have no known competing financial interests or personal relationships that could have appeared to influence the work reported in this paper.

References

Abarghani, A., Ostadhassan, M., Gentzis, T., Carvajal-Ortiz, H., Ocubalidet, S., Bubach, B.,

Mann, M., Hou, X., 2019. Correlating Rock-EvalTM Tmax with bitumen reflectance from organic petrology in the Bakken Formation. International Journal of Coal Geology 205, 87–104. https://doi.org/10.1016/j.coal.2019.03.003

Angradi, T.R., 1994. Trophic linkages in the lower Colorado River: multiple stable isotope evidence. Journal of the North American Benthological Society 13, 479–495.

Arthaud, F., Matte, P., 1977. Late Paleozoic strike-slip faulting in southern Europe and northern Africa: Result of a right-lateral shear zone between the Appalachians and the Urals. Geological Society of America Bulletin 88, 1305–1320.

Baird, D.W., 1967. The Permo-Carboniferous of southern Tunisia, in: Guidebook to the Geology and History of Tunisia. Petroleum Exploration Society of Libya, 9th Annual Field Conference. pp. 85–107.

Baudin, F., Disnar, J.-R., Aboussou, A., Savignac, F., 2015. Guidelines for Rock–Eval analysis of recent marine sediments. Organic Geochemistry 86, 71–80.

Behar, F., Beaumont, V., Penteado, H.D.B., 2001. Rock-Eval 6 technology: performances and developments. Oil & Gas Science and Technology 56, 111–134.

Ben Ayed, N., 1986. Évolution tectonique de l'avant-pays de la chaîne alpine de Tunisie du début du mésozoique à l'actuel (These de doctorat). Paris 11.

Ben Ferjani, F., Burrolet, P.F., Mejri, F., 1990. Petroleum geology of Tunisia: Entreprise Tunisienne des Activités Pétrolière (ETAP).

Ben Ismail, M.H., 1991. Les bassins mésozoïques (Trias à Aptien) du sud de la Tunisie: stratigraphie intégrée, caractéristiques géophysiques et évolution géodynamique. Unpublished doctoral thesis, Université de Tunis II 446.

Blanchart, P., 2011. Influences de l'oxydation et de la biodégradation anaérobie sur la matière organique de l'argile oligocène de Boom (Mol, Belgique) : Conséquences sur la formation d'espèces organiques hydrosolubles phd.thesis. Institut National Polytechnique de Lorraine.

Bodin, S., Petitpierre, L., Wood, J., Elkanouni, I., Redfern, J., 2010. Timing of early to mid-cretaceous tectonic phases along North Africa: New insights from the Jeffara escarpment (Libya–Tunisia). Journal of African Earth Sciences 58, 489–506.

Bouaziz A., Mabrouk El Asmi A., Skanji A., El Asmi K., (2015). A new borehole temperature adjustment in the Jeffara Basin (southeast Tunisia): Inferred source rock maturation and hydrocarbon generation via one-dimensional modeling. AAPG Bulletin, v. 99, no. 9 (September 2015), pp. 1649–1669.

Bouaziz, S., 1995. Etude de la tectonique cassante dans la plate-forme et lAtlas Saharien (Tunisie meridionale): volution des palochamps de contraintes et implication godynamique, Thse Doctorat PhD Thesis. University of Tunis II. Faculty of Sciences of Tunis.

Bouaziz, S., Barrier, E., Turki, M.M., Tricart, P., 1999. La tectonique permo-mésozoïque (anté-Vraconien) dans la marge sud téthysienne en Tunisie méridionale. Bulletin de la Société géologique de France 170, 45–56.

Busson, G., 1967. Mesozoique Saharien-1 Partie-L'Extreme-Sud Tunisien.

Carvajal-Ortiz, H., Gentzis, T., 2018. Geochemical screening of source rocks and reservoirs: The importance of using the proper analytical program. International Journal of Coal Geology, SI:TSOP/AASP/ICCP Houston 190, 56–69. https://doi.org/10.1016/j.coal.2017.11.014

Chaouachi, M.C., 1988. Etude sédimentologique des séries du Permien supérieur du Jebel Tebaga de Medenine (Sud-East de la Tunisie); genèse, diagenèse et potentiel réservoir des corps récifaux. Thèse 3e cycle, Fac. Sc. Tunis 285.

Chen, Z., Jiang, C., Lavoie, D., Reyes, J., 2016. Model-assisted Rock-Eval data interpretation for source rock evaluation: Examples from producing and potential shale gas resource plays. International Journal of Coal Geology 165, 290–302. https://doi.org/10.1016/j.coal.2016.08.026

Damsté, J.S.S., Kenig, F., Koopmans, M.P., Köster, J., Schouten, S., Hayes, J.M., de Leeuw, J.W., 1995. Evidence for gammacerane as an indicator of water column stratification. Geochimica et Cosmochimica Acta 59, 1895–1900.

Douvillé, H., 1933. M. Solignac, E. Berkaloff. Découverte du Permien marin au Djebel Tebaga (Extrême Sud Tunisien) C. R. Acad. Sciences 196, 21.

Driggs, A.F., 1977. The petrology of three Upper Permian bioherms, southern Tunisia (PhD Thesis). Brigham Young University.

Duvernoy, B., 1994. Tunisian and pelagian basin (Africa exploration opportunities; Vol. 13), in: Proceeding of the 4th Tunisian Petroleum Exploration Conference, Tunis.

Eglinton, G., Hamilton, R.J., 1967. Leaf epicuticular waxes. Science 156, 1322–1335.

Ehleringer, J.R., 1991. 13C/12C fractionation and its utility in terrestrial plant studies. Carbon isotope techniques 1, 187.

Espitalié, J., Deroo, G., Marquis, F., 1986. La pyrolyse Rock-Eval et ses applications. Troisième partie. Revue de l'Institut français du Pétrole 41, 73–89.

Espitalie, J., Madec, M., Tissot, B., 1980. Role of mineral matrix in kerogen pyrolysis: influence on petroleum generation and migration. AAPG Bulletin 64, 59–66.

Espitalié, J., Madec, M., Tissot, B., Mennig, J.J., Leplat, P., 1977. Source rock characterization method for petroleum exploration, in: Offshore Technology Conference. OnePetro.

Forsman, J.P., Hunt, J.M., 1958. Insoluble organic matter (kerogen) in sedimentary rocks. Geochimica et Cosmochimica Acta 15, 170–182.

Gabtni, H., 2006. Caractérisation profonde et modélisation géophysique des zones de transition entre les différents blocs structuraux de la Tunisie centro-méridionale. Université de Tunis El Manar, Thèse Doctorat 24.

Grasby, S.E., Beauchamp, B., 2008. Intrabasin variability of the carbon-isotope record across the Permian–Triassic transition, Sverdrup Basin, Arctic Canada. Chemical Geology 253, 141–150.

Hassen, M.B., Deffontaines, B., Turki, M.M., 2015. Analysis of Recent Deformation in the Southern Atlas of Tunisia Using Geomorphometry, in: Engineering Geology for Society and Territory-Volume 6. Springer, pp. 113–117.

Hazra, B., Dutta, S., Kumar, S., 2017. TOC calculation of organic matter rich sediments using Rock-Eval pyrolysis: Critical consideration and insights. International Journal of Coal Geology 169, 106–115. https://doi.org/10.1016/j.coal.2016.11.012

Hazra, B., Karacan, C.Ö., Tiwari, D.M., Singh, P.K., Singh, A.K., 2019. Insights from Rock-Eval analysis on the influence of sample weight on hydrocarbon generation from Lower Permian organic matter rich rocks, West Bokaro basin, India. Marine and Petroleum Geology 106, 160–170. https://doi.org/10.1016/j.marpetgeo.2019.05.006

Hazra, B., Singh, D.P., Chakraborty, P., Singh, P.K., Sahu, S.G., Adak, A.K., 2021. Using rock-eval S4Tpeak as thermal maturity proxy for shales. Marine and Petroleum Geology 127, 104977. https://doi.org/10.1016/j.marpetgeo.2021.104977

Hu, L., Shi, X., Guo, Z., Wang, H., Yang, Z., 2013. Sources, dispersal and preservation of sedimentary organic matter in the Yellow Sea: The importance of depositional hydrodynamic forcing. Marine Geology 335, 52–63. https://doi.org/10.1016/j.margeo.2012.10.008

Hunt, J.M., 1996. Petroleum Geochemistry and Geology, WH New York.

Jarvie, D.M., 2012. Shale resource systems for oil and gas: part 2—shale-oil resource systems. shale reservoirs—giant resources for the 21st century. Am. Assoc. Pet. Geol. Mem. Vol. 97, 89–119.

Jiamo, F., Guoying, S., Pingan, P., Brassell, S.C., Eglinton, G., Jigang, J., 1986. Peculiarities of salt lake sediments as potential source rocks in China. Organic Geochemistry 10, 119–126.

Karayigit, A.I., Oskay, R.G., Çelik, Y., 2021. Mineralogy, petrography, and Rock-Eval pyrolysis of late Oligocene coal seams in the Malkara coal field from the Thrace Basin (NW Turkey). International Journal of Coal Geology 244, 103814. https://doi.org/10.1016/j.coal.2021.103814

Khessibi, M., 1985. Etude sédimentologique des affleurements permiens du Djebel Tebaga de Médenine (Sud Tunisien). Bulletin des centres de recherches exploration-Production Elf-Aquitaine 9, 427–464.

Lafargue, E., Marquis, F., Pillot, D., 1998. Rock-Eval 6 applications in hydrocarbon exploration, production, and soil contamination studies. Revue de l'institut français du pétrole 53, 421–437.

Luo, G., Yang, H., Algeo, T.J., Hallmann, C., Xie, S., 2019. Lipid biomarkers for the reconstruction of deep-time environmental conditions. Earth-Science Reviews 189, 99–124.

Mathieu, G., 1949. Contribution à l'étude des monts troglodytes dans l'extrême Sud-Tunisien: géologie régionale des environs de Matmata medenine et Foum-Tatahouine. Verlag nicht ermittelbar.

Mejri, F., Burollet, P.F., Ferjani, A.B., 2006. Petroleum geology of Tunisia: A renewed synthesis. Enterprise tunisienne d'activités pétrolières.

Memmi, L., Burollet, P.F., Viterbo, I., 1986. Lexique stratigraphique de la Tunisie: première partie: Précambrien et Paléozoïque. Notes du Service géologique.

Meyers, P.A., 1997. Organic geochemical proxies of paleoceanographic, paleolimnologic, and paleoclimatic processes. Organic geochemistry 27, 213–250.

Meyers, P.A., 1997. Organic geochemical proxies of paleoceanographic, paleolimnologic, and paleoclimatic processes. Organic geochemistry 27, 213–250.

Moldowan, J.M., Dahl, J., Huizinga, B.J., Fago, F.J., Hickey, L.J., Peakman, T.M., Taylor, D.W., 1994. The molecular fossil record of oleanane and its relation to angiosperms. Science 265, 768–771.

Mraidi I., Mabrouk El Asmi A., Skanji A.., El Asmi K., Saidi M. (2021). New insights on source rock maturation in the southern Gulf of Gabes (Tunisia) via 1-D modeling: effect of combined corrected borehole temperature and thermal conductivity on heat flow distribution. Arabian Journal of Geosciences 14:773. https://doi.org/10.1007/s12517-021-07017-2

Niu, Z., Liu, G., Ge, J., Zhang, X., Cao, Z., Lei, Y., An, Y., Zhang, M., 2019. Geochemical characteristics and depositional environment of Paleogene lacustrine source rocks in the Lufeng Sag, Pearl River Mouth basin, South China Sea. Journal of Asian Earth Sciences 171, 60–77.

Ouaja, M., 2003. Etude sédimentologique et paléobotanique du Jurassique moyen-Crétacé inférieur du bassin de Tataouine (Sud-Est de la Tunisie) PhD Thesis. Lyon 1.

Pancost, R.D., Freeman, K.H., Patzkowsky, M.E., 1999b. Organic-matter source variation and the expression of a late Middle Ordovician carbon isotope excursion. Geology 27, 1015–1018.

Peters, K.E., Moldowan, J.M., 1991. Effects of source, thermal maturity, and biodegradation on the distribution and isomerization of homohopanes in petroleum. Organic geochemistry 17, 47–61.

Peters, K.E., Moldowan, J.M., 1993. The biomarker guide: interpreting molecular fossils in petroleum and ancient sediments.

Peters, K.E., Peters, K.E., Walters, C.C., Moldowan, J.M., 2005. The biomarker guide. Cambridge university press.

Qu, Y., Tao, H., Ma, D., Wu, T., Qiu, J., 2019. Biomarker characteristics and geological significance of middle and upper Permian source rocks in the southeastern Junggar Basin. Petroleum Science and Technology 37, 1–15. https://doi.org/10.1080/10916466.2019.1615950

Raji, M., Gröcke, D.R., Greenwell, H.C., Gluyas, J.G., Cornford, C., 2015. The effect of interbedding on shale reservoir properties. Marine and Petroleum Geology 67, 154–169.

Razgallah, S., Vachard, D., 1991. Systématique et biosedimentologie des algues constructrices permiennes Tubiphytes et Archaeolithoporella suivant l'exemple du Jebel Tebaga (Murghabien de Tunisie). Palaeontographica Abteilung B Paläophytologie 221, 171–205.

Romero-Sarmiento, M.-F., 2019. A quick analytical approach to estimate both free versus sorbed hydrocarbon contents in liquid-rich source rocks. AAPG Bulletin 103, 2031–2043.

Romero-Sarmiento, M.-F., Euzen, T., Rohais, S., Jiang, C., Littke, R., 2016a. Artificial thermal maturation of source rocks at different thermal maturity levels: Application to the Triassic Montney and Doig formations in the Western Canada Sedimentary Basin. Organic Geochemistry 97, 148–162.

Romero-Sarmiento, M.-F., Pillot, D., Letort, G., Lamoureux-Var, V., Beaumont, V., Huc, A.-Y., Garcia, B., 2016b. New Rock-Eval method for characterization of unconventional shale resource systems. Oil & Gas Science and Technology–Revue d'IFP Energies nouvelles 71, 37.

Romero-Sarmiento, M.F., Pillot, D., Letort, G., Lamoureux-Var, V., Beaumont, V., Huc, A.Y., Garcia, B., 2014a. New Rock-Eval method for characterization of shale plays, in: 14th Latin American Congress on Organic Geochemistry (ALAGO), Buzios, Rio de Janeiro, Brazil.

Romero-Sarmiento, M.-F., Ramiro-Ramirez, S., Berthe, G., Fleury, M., Littke, R., 2017. Geochemical and petrophysical source rock characterization of the Vaca Muerta Formation, Argentina: Implications for unconventional petroleum resource estimations. International Journal of Coal Geology 184, 27–41.

Romero-Sarmiento, M.-F., Rouzaud, J.-N., Bernard, S., Deldicque, D., Thomas, M., Littke, R., 2014b. Evolution of Barnett Shale organic carbon structure and nanostructure with increasing maturation. Organic Geochemistry 71, 7–16.

Scheeder, G., Weniger, P., Blumenberg, M., 2020. Geochemical implications from direct Rock-Eval pyrolysis of petroleum. Organic Geochemistry 146, 104051. https://doi.org/10.1016/j.orggeochem.2020.104051

Song, J., Littke, R., Weniger, P., 2017. Organic geochemistry of the lower Toarcian Posidonia Shale in NW Europe. Organic Geochemistry 106, 76–92.

Soucémarianadin, L., Cécillon, L., Guenet, B., Chenu, C., Baudin, F., Nicolas, M., Cyril, G., Barré, P., 2018. Environmental factors controlling soil organic carbon stability in French forest soils. Plant and Soil 426, 1–20. https://doi.org/10.1007/s11104-018-3613-x.

Spiro, S., Guest, J.R., 1991. Adaptive responses to oxygen limitation inEscherichia coli. Trends in Biochemical Sciences 16, 310–314. https://doi.org/10.1016/0968-0004(91)90125-F

Termier, H., 1977. Monographie paléontologique des affleurements Permiens du Djebel Tébaga (sud Tunisien).

Tissot, B.P., Welte, D.H., 1984. Geochemical fossils and their significance in petroleum formation, in: Petroleum Formation and Occurrence. Springer, pp. 93–130.

Touati, M.A., Rodgers, M.R., 1998. Tectono-stratigraphic history of the Southern Gulf of Gabes and the hydrocarbon habitats, in: Proceedings of the Sixth Tunisian Exploration and Production Conference (Tunis, May: 5–9). pp. 343–370.

Underdown, R., Redfern, J., 2008. Petroleum generation and migration in the Ghadames Basin, North Africa: a two-dimensional basin-modeling study. American Association of Petroleum Geologists Bulletin 92, 53–76.

Vu, T.T.A., Horsfield, B., Mahlstedt, N., Schenk, H.J., Kelemen, S.R., Walters, C.C., Kwiatek, P.J., Sykes, R., 2013. The structural evolution of organic matter during maturation of coals and its impact on petroleum potential and feedstock for the deep biosphere. Organic Geochemistry 62, 17–27. https://doi.org/10.1016/j.orggeochem.2013.06.011

Whiticar, M.J., 1996. Stable isotope geochemistry of coals, humic kerogens and related natural gases. International Journal of Coal Geology 32, 191–215.

Yang, C., Wilkinson, G.M., Cole, J.J., Macko, S.A., Pace, M.L., 2014. Assigning hydrogen, carbon, and nitrogen isotope values for phytoplankton and terrestrial detritus in aquatic food web studies. Inland Waters 4, 233–242.

Yang, S., Horsfield, B., 2020. Critical review of the uncertainty of Tmax in revealing the thermal maturity of organic matter in sedimentary rocks. International Journal of Coal Geology 225, 103500. https://doi.org/10.1016/j.coal.2020.103500

Zaafouri, A., Haddad, S., Mannaî-Tayech, B., 2017. Subsurface Permian reef complexes of southern Tunisia: Shelf carbonate setting and paleogeographic implications. Journal of African Earth Sciences 129, 944–959.

Table 1

Well	Depth (m)	Lithology	Sh0(mgHC/g)	Sh1(mgHC/g)	Sh2(mgHC/g)	S3 (mg/g)	HCcont(mg/g)	HQI(wt.%)	TmaxSh2(°C)	TOC(%)	HI(mgHC/gTOC)	PP(Sh0+sh1)+sh2	Sh2/S3

D1-S$_1$	1549	M-C	0.63	19.88	10.95	13.92	20.51	3.07	406	7.76	141	31.46	0.79
D1-S$_2$	2144	M-C	0.56	1.21	10.68	2.05	1.77	31.64	435	4.85	220	12.45	5.21
D1-S$_3$	2159	M-C	0.08	0.36	2.38	1.79	0.44	18.18	437	1.84	129	2.82	1.33
D1-S$_4$	2282	M	0.06	0.43	2.05	2.31	0.49	12.24	439	1.17	175	2.54	0.89
D1-S$_5$	2393	M	0.02	0.29	1.03	1.36	0.31	6.45	436	1.12	92	1.34	0.76
D1-S$_6$	3639	M	0.06	0.50	1.74	3.06	0.56	10.71	431	1.93	90	2.30	0.57
D1-S$_7$	3932	M	0.02	0.17	0.53	1.58	0.19	10.53	424	1.14	46	0.72	0.34
D1-S$_8$	3950	M	0.01	0.05	0.22	1.25	0.06	16.67	429	0.57	39	0.28	0.18
D1-S$_9$	4052	M	0.02	0.13	0.34	1.18	0.15	13.33	424	0.69	49	0.49	0.29
D2-S$_1$	1083	C	0.01	0.09	0.35	0.78	0.10	10.00	428	0.50	70	0.45	0.45
D2-S$_2$	1175	C	0.04	0.64	11.82	2.02	0.68	5.88	416	5.54	213	12.50	5.85
D2-S$_3$	1240	C	0.09	0.75	6.42	1.44	0.84	10.71	426	3.01	213	7.26	4.46
D2-	12	C	0.34	1.28	11.07	1.08	1.62	20.99	421	4.01	276	12.69	10.2

S_4	92												5
D2-S_5	1360	C	0.06	0.35	2.67	0.87	0.41	14.63	429	1.27	210	3.08	3.07
D2-S_6	1564	M-C	0.03	0.16	1.48	0.99	0.19	15.79	437	1.13	131	1.67	1.49
D2-S_7	1618	M-C	0.02	0.08	0.79	0.95	0.10	20.00	436	1.25	63	0.89	0.83
D2-S_8	1700	C	0.05	0.25	2.02	0.78	0.30	16.67	439	1.30	155	2.32	2.59
D2-S_9	1748	C	0.07	0.42	2.81	0.80	0.49	14.29	436	1.44	195	3.30	3.51
D2-S_{10}	1948	C	0.20	0.90	7.32	0.87	1.10	18.18	442	3.35	219	8.42	8.41
D2-S_{11}	2036	M-C	0.13	0.41	2.16	0.64	0.54	24.07	443	1.15	188	2.70	3.38
D2-S_{12}	2068	M	0.04	0.17	1.02	0.89	0.21	19.05	442	0.88	116	1.23	1.15
D2-S_{13}	2096	M-C	0.17	0.50	3.17	0.58	0.67	25.37	443	1.57	202	3.84	5.47
D2-S_{14}	2140	C	0.02	0.10	0.51	0.92	0.12	16.67	442	0.71	72	0.63	0.55
D2-S_{15}	2212	M	0.01	0.07	0.31	0.80	0.08	12.50	441	0.47	66	0.39	0.39
D2-S_{16}	2404	M-C	0.05	0.22	0.86	0.64	0.27	18.52	455	0.93	92	1.13	1.34

D2-S17	2412	M	0.05	0.18	0.78	0.58	0.23	21.74	449	0.64	122	1.01	1.34
D2-S18	2542	M	0.04	0.19	0.54	0.60	0.23	17.39	457	0.79	68	0.77	0.90
D2-S19	2588	M-C	0.02	0.11	0.46	0.50	0.13	15.38	454	0.57	81	0.59	0.92
J1-S1	2262	M-C	0.01	0.02	0.05	0.76	0.03	33.33	382	0.10	50	0.08	0.07
J1-S2	2263	M-C	0.00	0.01	0.04	0.65	0.01	0.00	457	0.11	36	0.05	0.06
J1-S3	2269	M	0.01	0.06	0.34	0.66	0.07	14.29	555	1.32	26	0.41	0.52
J1-S4	2270	M	0.01	0.02	0.09	0.58	0.03	33.33	562	0.44	20	0.12	0.16
J1-S5	2273	M	0.01	0.03	0.12	0.83	0.04	25.00	550	0.52	23	0.16	0.14
J1-S6	2274	M	0.01	0.05	0.10	0.73	0.06	16.67	567	0.54	19	0.16	0.14
J1-S7	2297	M	0.01	0.04	0.11	0.60	0.05	20.00	538	0.32	34	0.16	0.18
J1-S8	2305	M	0.01	0.03	0.09	0.74	0.04	25.00	556	0.48	19	0.13	0.12
J1-S9	2306	M	0.01	0.04	0.15	0.80	0.05	20.00	548	0.86	17	0.20	0.19
J1-	24	M-C	0.00	0.02	0.05	0.65	0.02	0.00	499	0.31	16	0.07	0.08

S_{10}	1525												
J1-S_{11}	2525	M-C	0.00	0.03	0.04	0.68	0.03	0.00	416	0.11	36	0.07	0.06
J1-S_{12}	2614	M-C	0.01	0.02	0.05	0.56	0.03	33.33	409	0.17	29	0.08	0.09
J1-S_{13}	2738	C	0.01	0.03	0.06	0.53	0.04	25.00	404	0.21	29	0.10	0.11
J1-S_{14}	3210	C	0.00	0.03	0.05	0.63	0.03	0.00	383	0.18	28	0.08	0.08
J1-S_{15}	3366	C	0.02	0.04	0.10	0.92	0.06	33.33	578	0.57	18	0.16	0.11
J1-S_{16}	3400	C	0.01	0.04	0.13	0.83	0.05	20.00	412	0.30	43	0.18	0.16
J2-S_{1}	986	C	0.02	0.20	4.44	1.76	0.22	9.09	432	3.24	137	4.66	2.52
J2-S_{2}	1000	C	0.02	0.11	1.26	1.71	0.13	15.38	431	1.49	85	1.39	0.74
J2-S_{3}	1018	C	0.07	0.39	3.82	1.40	0.46	15.22	435	4.12	93	4.28	2.73
J2-S_{4}	1038	C	0.16	1.00	9.30	1.97	1.16	13.79	431	7.69	121	10.46	4.72
J2-S_{5}	1060	M-C	0.01	0.12	0.64	1.10	0.13	7.69	433	1.37	47	0.77	0.58
J2-S_{6}	1122	C	0.06	0.46	6.21	0.99	0.52	11.54	431	3.06	203	6.73	6.27
J	1	C	0.04	0.36	3.66	0.8	0.40	10.	433	2.	169	4.06	4.

2-S$_7$	136					2		00		17			46
J2-S$_8$	1138	C	0.07	0.50	5.70	1.23	0.57	12.28	431	2.79	204	6.27	4.63
J2-S$_9$	1206	C	0.12	0.63	5.72	1.12	0.75	16.00	437	2.61	219	6.47	5.11
J2-S$_{10}$	1214	C	0.05	0.26	2.51	1.15	0.31	16.13	438	1.47	171	2.82	2.18
J2-S$_{11}$	1220	C	0.12	0.73	7.80	1.42	0.85	14.12	437	4.17	187	8.65	5.49
J2-S$_{12}$	1224	C	0.05	0.36	3.16	1.22	0.41	12.20	436	2.31	137	3.57	2.59
J2-S$_{13}$	1226	C	0.09	0.57	4.16	1.32	0.66	13.64	436	2.81	148	4.82	3.15
J2-S$_{14}$	1264	C	0.18	0.57	5.72	1.00	0.75	24.00	433	2.03	282	6.47	5.72
J2-S$_{15}$	1270	C	0.09	0.47	3.51	1.15	0.56	16.07	434	1.72	204	4.07	3.05
J2-S$_{16}$	1280	M-C	0.12	0.59	4.21	0.98	0.71	16.90	433	2.06	204	4.92	4.30
J2-S$_{17}$	1284	C	0.14	0.75	6.22	1.07	0.89	15.73	434	2.98	209	7.11	5.81
J2-S$_{18}$	1290	C	0.08	0.51	5.44	1.18	0.59	13.56	436	2.95	184	6.03	4.61
J2-S$_{1}$	130	M-C	0.02	0.13	1.30	1.18	0.15	13.33	439	1.65	79	1.45	1.10

$_{9}$	4												
J 2-S$_{20}$	1395	C	0.39	1.41	9.75	1.14	1.80	21.67	432	4.46	219	11.55	8.55
J 2-S$_{21}$	1410	C	0.91	2.44	17.03	1.32	3.35	27.16	431	6.95	245	20.38	12.90
J 2-S$_{22}$	1425	C	0.07	0.29	2.64	0.97	0.36	19.44	440	1.64	161	3.00	2.72
J 2-S$_{23}$	1430	C	0.56	1.81	13.79	1.07	2.37	23.63	436	4.69	294	16.16	12.89
J 2-S$_{24}$	1450	C	0.42	1.20	7.07	0.86	1.62	25.93	438	2.72	260	8.69	8.22
J 2-S$_{25}$	1488	C	0.22	1.24	10.30	1.01	1.46	15.07	441	3.80	271	11.76	10.20
J 2-S$_{26}$	1490	C	0.20	1.93	18.95	1.08	2.13	9.39	434	6.69	283	21.08	17.55
J 2-S$_{27}$	1495	C	0.19	1.37	13.04	1.07	1.56	12.18	436	5.00	261	14.60	12.19
J 2-S$_{28}$	1560	C	0.05	0.48	4.90	0.97	0.53	9.43	450	3.51	140	5.43	5.05
J 2-S$_{29}$	1576	M-C	0.06	0.31	3.21	1.15	0.37	16.22	442	2.75	117	3.58	2.79
J 2-S$_{30}$	1643	M	0.05	0.30	2.44	0.87	0.35	14.29	441	1.45	168	2.79	2.80

Abbreviations: HCcont = hydrocarbon content index. **TOC**: total organic carbon (%). **Tmax**: S2 maximum peak temperature (°C). **PP**: Petroleum potential ((SH0+SH1+SH2) mg HC.g/rock). **IH:** Hydrogen Index..

M=Marl**, C=**clay

Table 2

Samples	Lithology	Age	Depth(m)
D1-S4	M	Permian	2282
D1-S5	M	Permian	2393
D2-S16	M-C	Permian	2404
Fegaguira	C	Upper Silurian-	3838
Azzel	C	Ordovician	3913

Abbreviations: **M**=Marl, **C**=clay

Table 3

			Before acid attack		After acid attack				
Well	Depth (m)	Age	TOC(%)	MINC(%)	TOC(%)	MINC(%)	C(%)	$\delta^{13}C$ (‰)	σ
D1-S_2	2144	Permian	4.85	8.77	14.88	0.50	15.17	-22.65	0.02
D1-S_3	2159	Permian	1.84	8.47	15.16	0.87	15.59	-18.95	0.016971
D1-S_4	2282	Permian	1.17	9.14	9.78	0.61	9.64	-25.21	0.019092
D1-S_5	2393	Permian	1.12	8.04	3.75	0.45	3.52	-24.01	0.243245
D1-S_6	3639	Permian	1.93	8.48	2.54	0.42	2.29	-23.90	0.147078
D2-S_2	1175	Permian	5.54	7.25	9.74	0.66	9.97	-21.83	0.021213
D2-S_3	1240	Permian	3.01	7.66	7.39	0.50	6.57	-23.72	0.03677
D2-S_4	1292	Permian	4.01	8.08	12.39	0.65	13.74	-23.24	0.104652
D2-S_{10}	1948	Permian	3.35	7.83	6.93	0.33	7.19	-26.28	0.02545584
D2-S_{13}	2096	Permian	1.57	8.18	11.83	0.29	12.12	-22.62	0.062933
J1-S_3	2269	Permian	1.32	7.36	2.13	0.47	1.85	-22.12	0.017678
J1-S_5	2273	Permian	0.52	3.43	0.67	0.41	0.58	-23.69	0.136472

J1-S_6	2274	Permian	0.54	7.63	1.95	0.39	2.22	-21.95	0.206475
J1-S_9	2306	Permian	0.86	6.48	1.58	0.35	1.39	-24.23	0.55861436
J1-S_{15}	3366	Permian	0.57	7.29	1.87	0.26	1.60	-24.53	0.097581
J2-S_1	986	Permian	3.24	6.67	0.92	0.39	1.09	-19.18	0.155563
J2-S_4	1038	Permian	7.69	5.68	2.78	0.35	3.02	-21.45	0.25668
J2-S_{11}	1220	Permian	4.17	7.14	5.44	0.27	5.40	-21.80	0.083439
J2-S_{21}	1410	Permian	6.95	8.27	12.75	0.38	13.16	-20.72	0.106773
J2-S_{26}	1490	Permian	6.69	7.91	15.26	0.31	15.89	-21.36	0.067882

. **TOC**: total organic carbon (%). **MINC** =Mineral carbon (%)

Table 4

Parameters	**Fegaguira**	**Azzel**	**D2-S_{16}**	**D1-S_4**	**D1-S_5**
% C27	45	43	30	34	38
% C28	23	28	21	10	8
% C29	31	29	30	55	53
C19 tr/(C19 tr+C23 tr)	0.06	0.19	0.28	0.25	0.4
C22tr/C21tr	0.23	0.27	0.62	0.24	0.24
C23 tr/H30	4.06	1.99	0.5	0.14	0.1
C24Tet/ (C24 Tet+C23 tr)	0.16	0.1	0.28	0.46	0.47
C24Tet/ C26tr	0.38	0.25	0.86	3.29	2.81
C24tr/C23tr	0.61	0.61	0.48	0.51	0.55
C26tr/C25tr	0.09	1.05	0.91	0.49	0.66
C27βα Dia/C27ββ S Stéranes	1.34	1.44	0.49	0.5	0.68
C29/C30HH	0.7	0.79	0.82	0.52	0.53
C29S/(S+R) stéranes	0.59	0.6	0.39	0.49	0.5
C29ββ/C29 (αα+ββ) stéranes	0.59	0.6	0.39	0.53	0.55
C31R/H	0.24	0.25	0 .38	0.34	0.46
C35/C34	0.56	0.5	0.88	0.47	0.69
C35HH/C34HH	0.5	0.56	0.88	0.47	0.69
Gammacérane/hopane	0.13	0.24	0.05	0.05	0.03
Ph/nC18	0.4	0.59	0.35	0.28	1.03
Pr/nC17	0.37	0.5	0.43	0.43	0.69
Pr/Ph	1.08	1.15	1.51	0.74	1.07
Ts/Tm	2.68	1.94	0.67	0.52	0.7

%C27=100*C27ββ(R+S)/ (C27ββ(R+S) +C28ββ(R+S) +C29ββ(R+S)): m/z 218
%C28=100*C28ββ(R+S)/ (C27ββ(R+S) +C28ββ(R+S) +C29ββ(R+S)): m/z 218
%C29=100*C29ββ(R+S)/ (C27ββ(R+S) +C28ββ(R+S) +C29ββ(R+S)): m/z 218

Figures captions

Fig. 1 (A) Digital Elevation Model (DEM) of Mediterranean Sea domain. Boxed area indicates location of the Tunisia region (Alyahyaoui.,et al 2015) and (B) Digital elevation model of the south-eastern of Tunisia indicating the location study area (1: Mediterranean Sea, 2: SE Jeffara Basin, 3: Dahar, 4: Jebel Tebaga, 5: Chotts area of the North Range (modified from Bouaziz., et al 1995).

Fig. 2 Late Hercynian unconformity subcrop map of southern Tunisia (Modified from Memmi et al., 1986).

Fig. 3 Location map of studied wells.

Fig.4 Pyrograms obtained by Rock-Eval® Shale Play™ method for one selected sample (J2-S_{26}), illustrating that this method provide a good assessment of free and/or retained hydrocarbons in rock sample.

Fig.5 Free and/or sorbed liquid hydrocarbon content [HCcont] versus TOC content from D1-S5 source rock samples (modified from Romero-Sarmiento et al., 2016a).

Fig. 6 Parameters obtained by Rock-Eval® Shale Play™ and for D1 studied samples.

Fig.7 Parameters obtained by Rock-Eval® Shale Play™ and for J2 studied samples.

Fig.8 Parameters obtained by Rock-Eval® Shale Play™ and for J1 studied samples.

Fig.9 Parameters obtained by Rock-Eval® Shale Play™ and for D1 studied samples.

Fig.10 (A)-HI/ TOC, (B)-SH2/S3 / TOC shows potential generation of the" D1, J2, J1 and D2 of the Permian.

Fig.11 HI / T_{max}, showing the type of showing stages of maturity and organic matter contained in the Permian source rocks of the wells.

Fig.12 (A)-3D block diagram of the crustal thinning of the crust on glove-finger form on the Jeffara, (B)-a synthetic model of a collapse at the sedimentary weft after a significant rifting associated to a mantle rise (Gabtni.,2006) and (C)-Map of geothermal flux changes (Della Vedova et al., 1995in Gabtni,2006) (above) and average geothermal gradient (expressed in °c/100m) (in the bottom) in the Jeffara region.

Fig.13 (A)-HI / IO and SH 2 / Toc showing the type of organic matter contained in the Permian source rocks.

Fig.14 Rock samples studied from different wells D1, J2, J1 and D1 from the Jeffara area showing the percentages of MINC (A) and the percentages of organic carbon content (B) before and after isolation of organic matter (OM) obtained by conventional acid attack following IFPEN procedures (Durand and Nicaise, 1980).

Fig.15 Relationship between TOC and $\delta^{13}C$ (‰) of organic matter between different Permian wells.

Fig.16 HI (kerogen and maturity dependent) plot versus carbon isotope ratios of organic matter in Permian source rocks from wells D1, J2, J1 and D1. (Raja et al., 2015).

Fig.17 Comparison $\delta^{13}C$ (‰) of organic matter values between the kerogen of potential source rock (liu et al., 2012).

Fig.18 Relationship between TOC from Elemental Analysis (%) and TOC from Rock-Eval® Shale PlayTM (%) of organic matter of different D1-S5 wells.

Fig.19 Relationship between TOC and $\delta^{13}C$ (‰) of organic matter.

Fig.20 GC/MS TIC distribution characteristics of samples Azzel, Fegaguira (D1-S4-D1-S5) and D2-S16.

Fig.21 Partial mass fragmentograms of aliphatic hydrocarbon fraction showing the distribution of terpanes/hopanes (m/z 191) and steranes (m/z 217) of selected samples from the Permian.

Fig.22 Ternary diagram based on the composition of C_{27}%, C_{28}%, C_{29}% steranes showing the origin and the deposition medium of the organic matter of the samples Azzel, Fegaguir, (D1-S4-D1-S5) and D2-S16 .

Fig.23 Diagram of the Pristane / n-C_{17} ratio versus the Phytane / n-C_{18} ratio showing the deposition medium of the organic matter contained in the samples Azzel, Fegaguira sources of Dahare area and D1 of Jeffara.

Fig.24 (A)C_{26}tr / C_{25}tr diagram versus C_{31}R/C_{30} Hopanes of samples Azzel, Fegaguira, D2-S16, D1-S_4 and D1- S_5 .(B) Diagram $C_{27}\beta\alpha$ dia / $C_{27}\beta\beta$ s steranes as a function of C_{29} / C_{30} hopanes relating to samples Azzel, Fegaguira, D2-S16 and (D1-S_4, D1-S_5).

Fig.25 Diagram $C_{29}\beta\beta$ / C_{29} ($\alpha\alpha$ + $\beta\beta$) steranes as a function of C_{29} $\alpha\alpha$20s / (20s + 20r) steranes of Azzel, Fegaguira And Permian samples D2-S16, D1-S_4 and D1-S_5.

Table captions

Table 1 Bulk parameters obtained by the Rock-Eval® Shale Play™ method for studied D1-S5 samples in well D1, J2, J1 and D1.

Table 2 sources rocks samples investigated from southern Tunisia in the Azzel, Fegaguira, and Permian source rocks

Table 3 TOC and MINC before and after acid attack, organic carbon isotope ($\delta 13C_{org}$) and elemental composition (C %) of the 20 selected samples of D1-S5.

Table 4 Biomarkers parameters based on GC-MS results of the source rock Azzel, Fegaguira, D2-S16, D1-S_4 and D1-S_5.

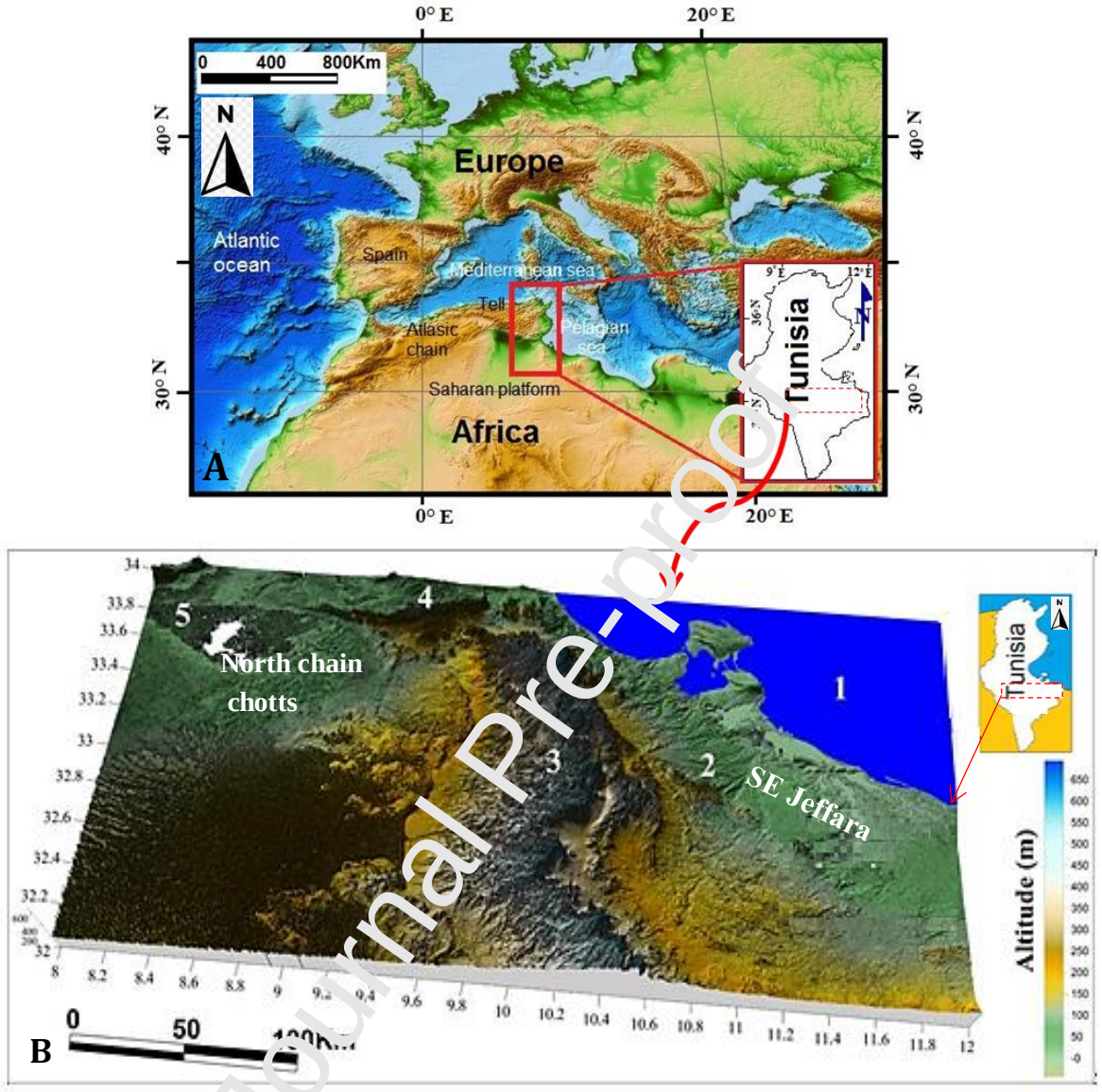

Figure 1

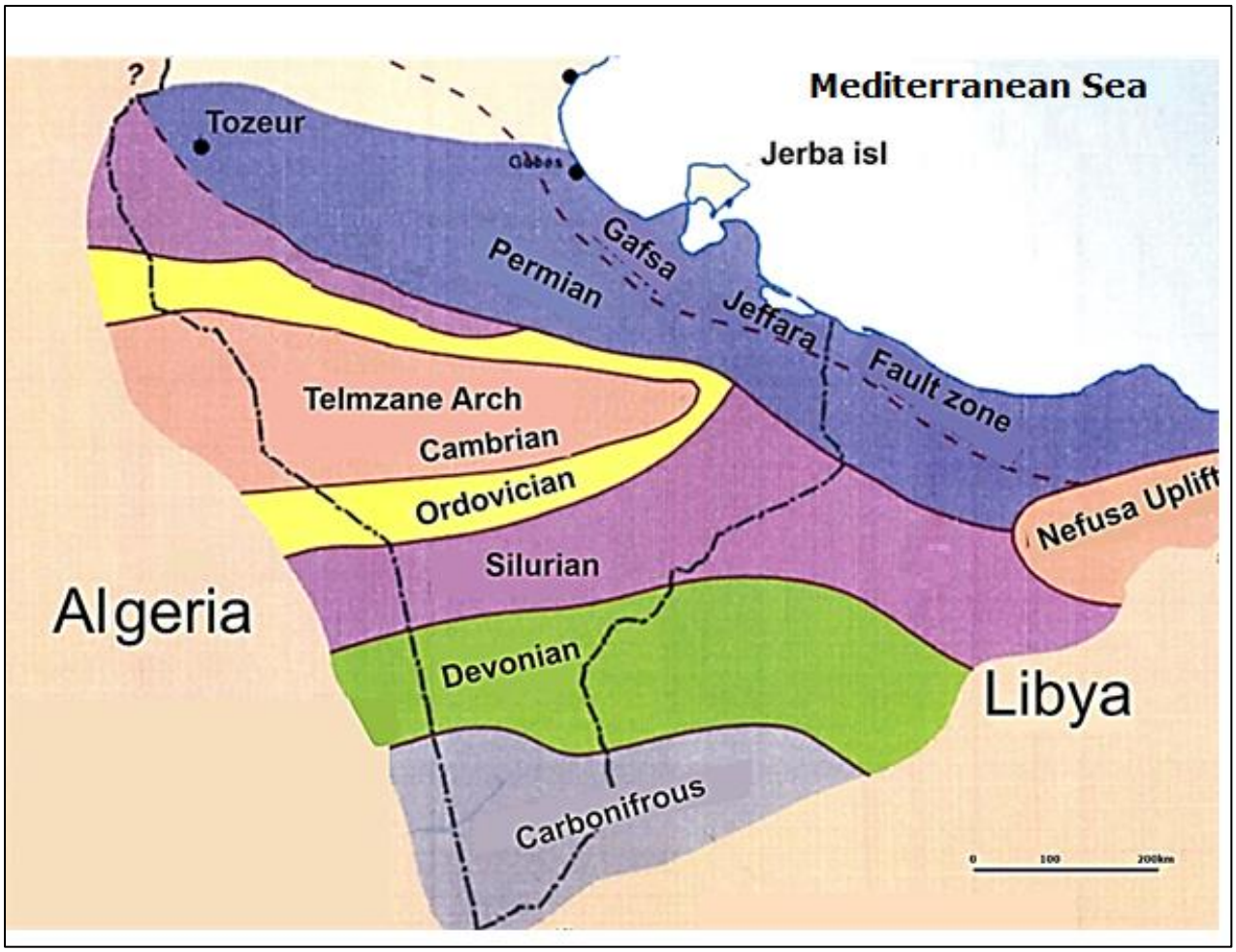
Mediterranean Sea
Tozeur
Gabes
Jerba isl
Gafsa
Permian
Jeffara
Fault zone
Telmzane Arch
Cambrian
Ordovician
Nefusa Uplift
Silurian
Algeria
Devonian
Libya
Carbonifrous
0
100
200km

Figure 2

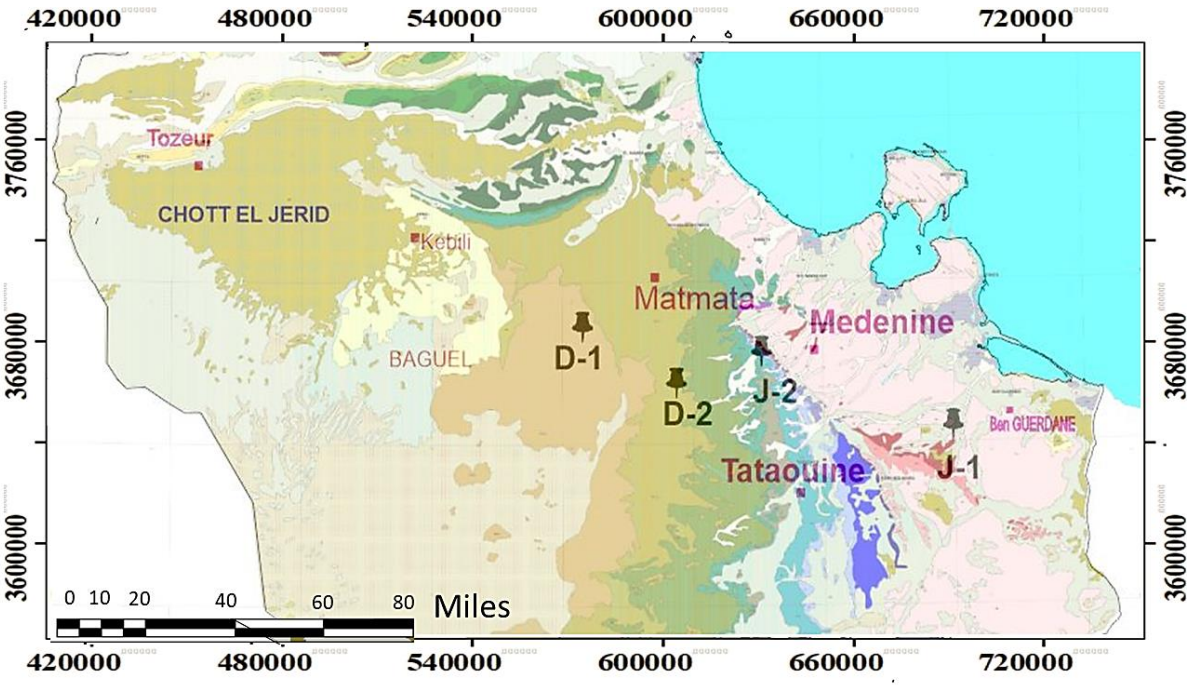

Figure 3

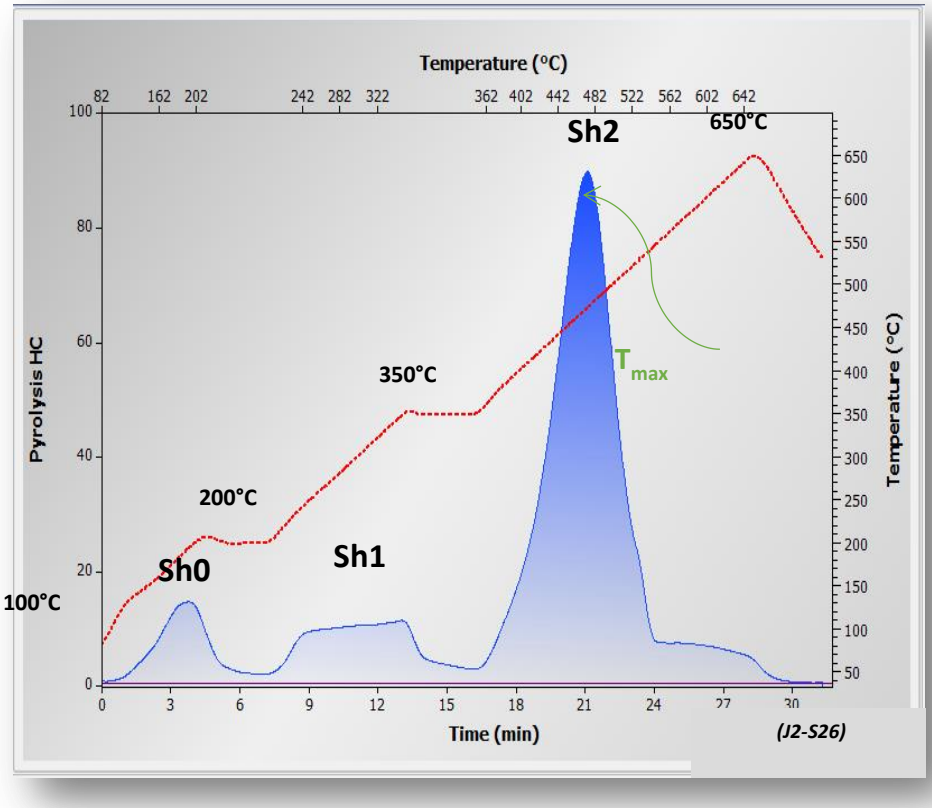

Figure 4

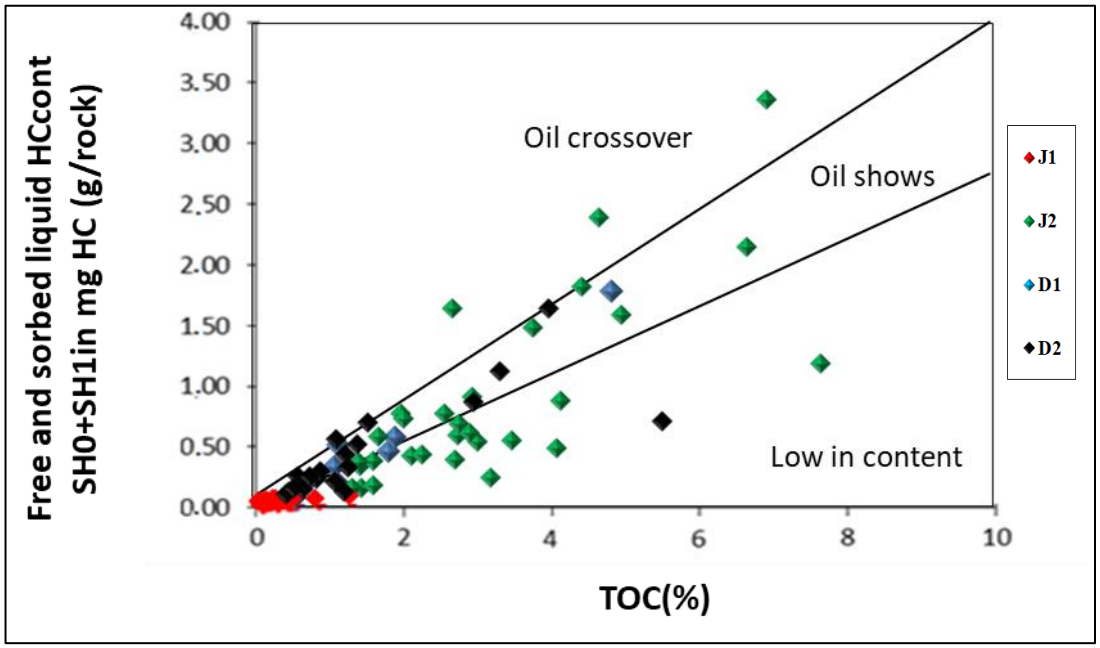
Free and sorbed liquid HCcont
SH0+SH1in mg HC (g/rock)
4.00
3.50
3.00
2.50
2.00
1.50
1.00
0.50
0.00
0
2
4
6
8
10
TOC(%)
Oil crossover
Oil shows
Low in content
J1
J2
D1
D2

Figure 5

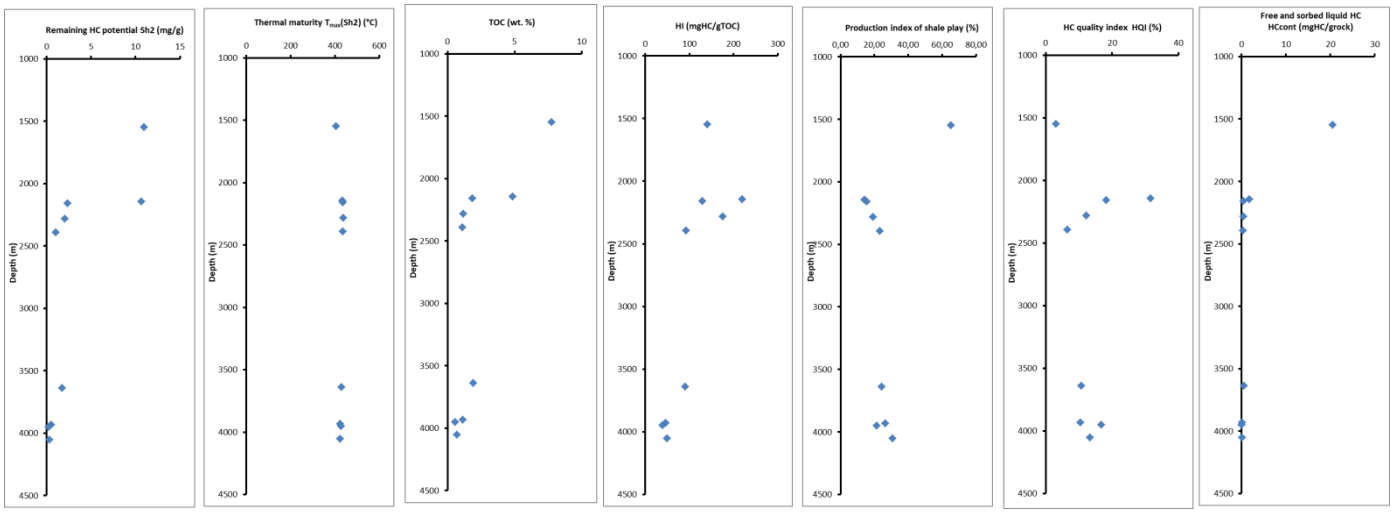

Figure 6

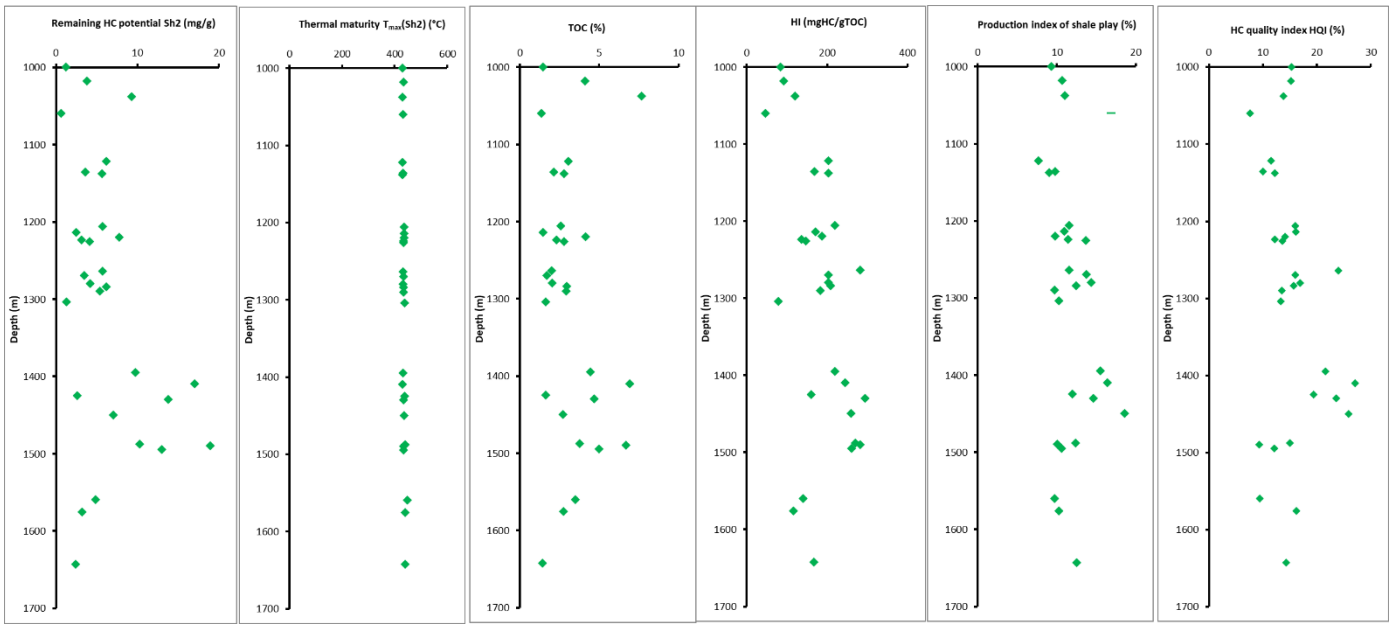

Figure 7

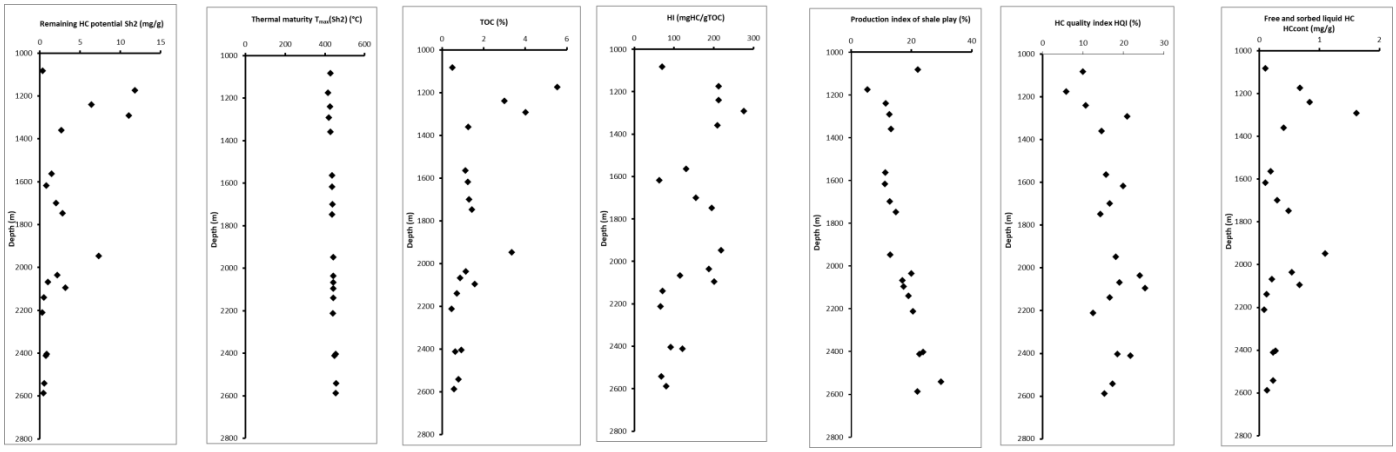

Figure 8

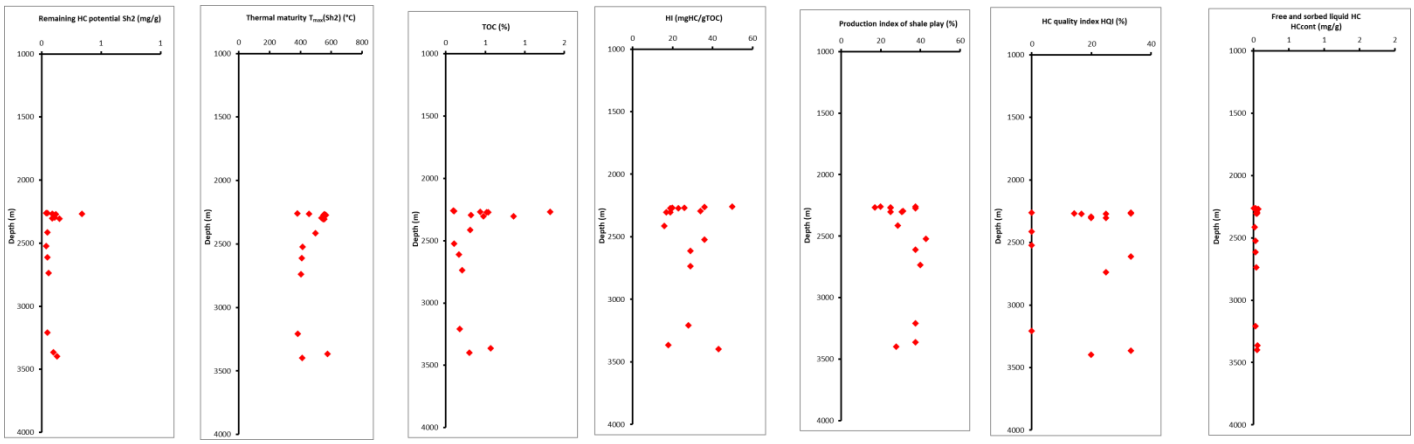

Figure 9

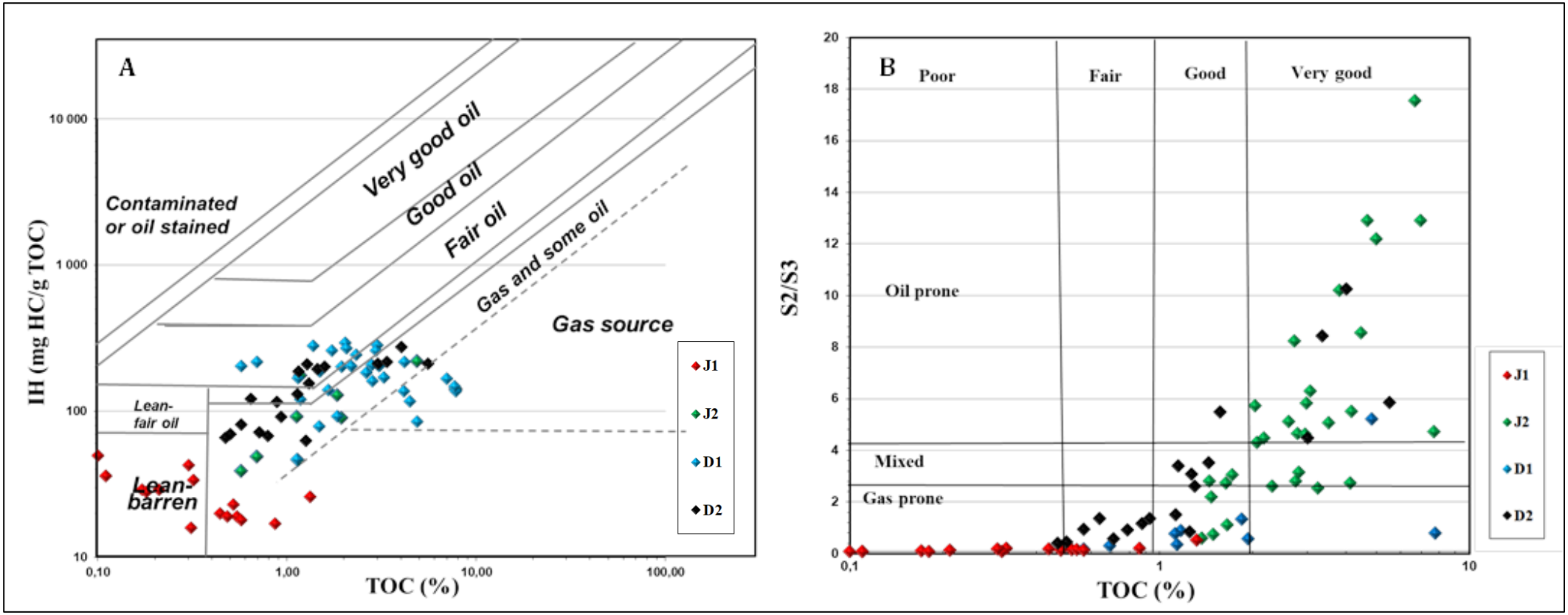
A
Contaminated or oil stained
Very good oil
Good oil
Fair oil
Gas and some oil
Gas source
Lean-fair oil
Lean-barren
IH (mg HC/g TOC)
TOC (%)
J1
J2
D1
D2
B
Poor
Fair
Good
Very good
Oil prone
Mixed
Gas prone
S2/S3
TOC (%)

Figure 10

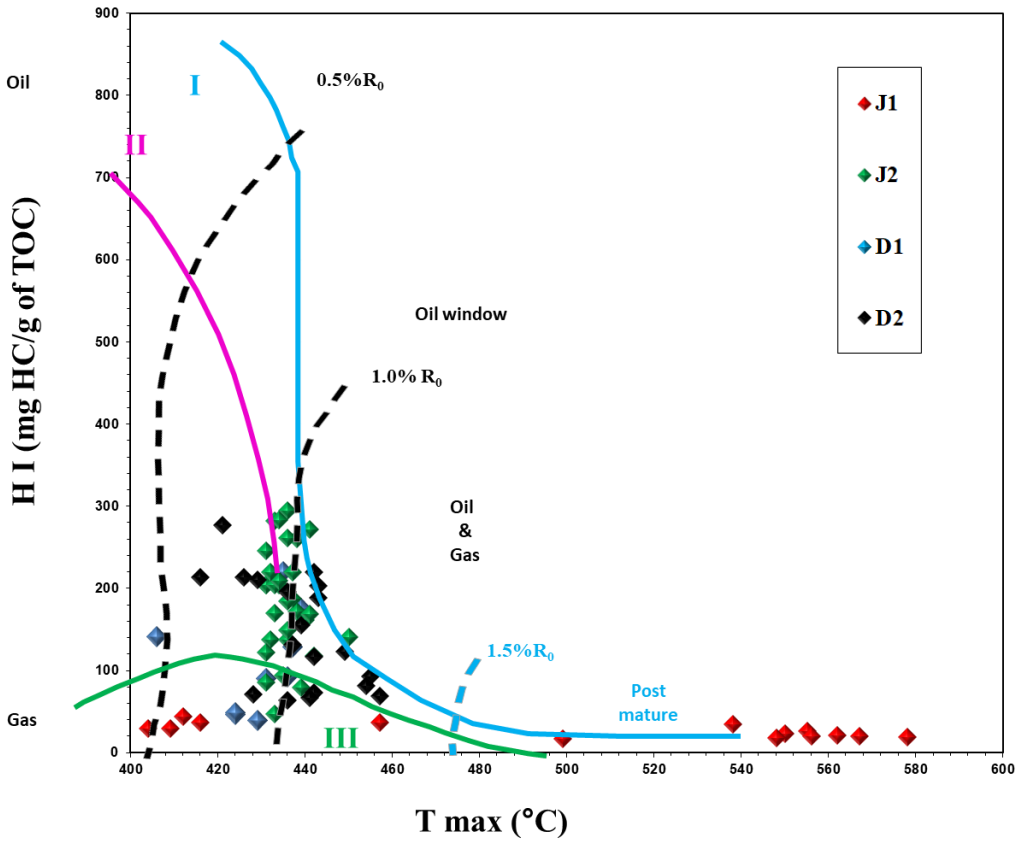
Oil
Gas
H I (mg HC/g of TOC)
T max (°C)
I
II
III
0.5%R0
1.0% R0
1.5%R0
Oil window
Oil
&
Gas
Post
mature
J1
J2
D1
D2
900
800
700
600
500
400
300
200
100
0
400
420
440
460
480
500
520
540
560
580
600

Figure 11

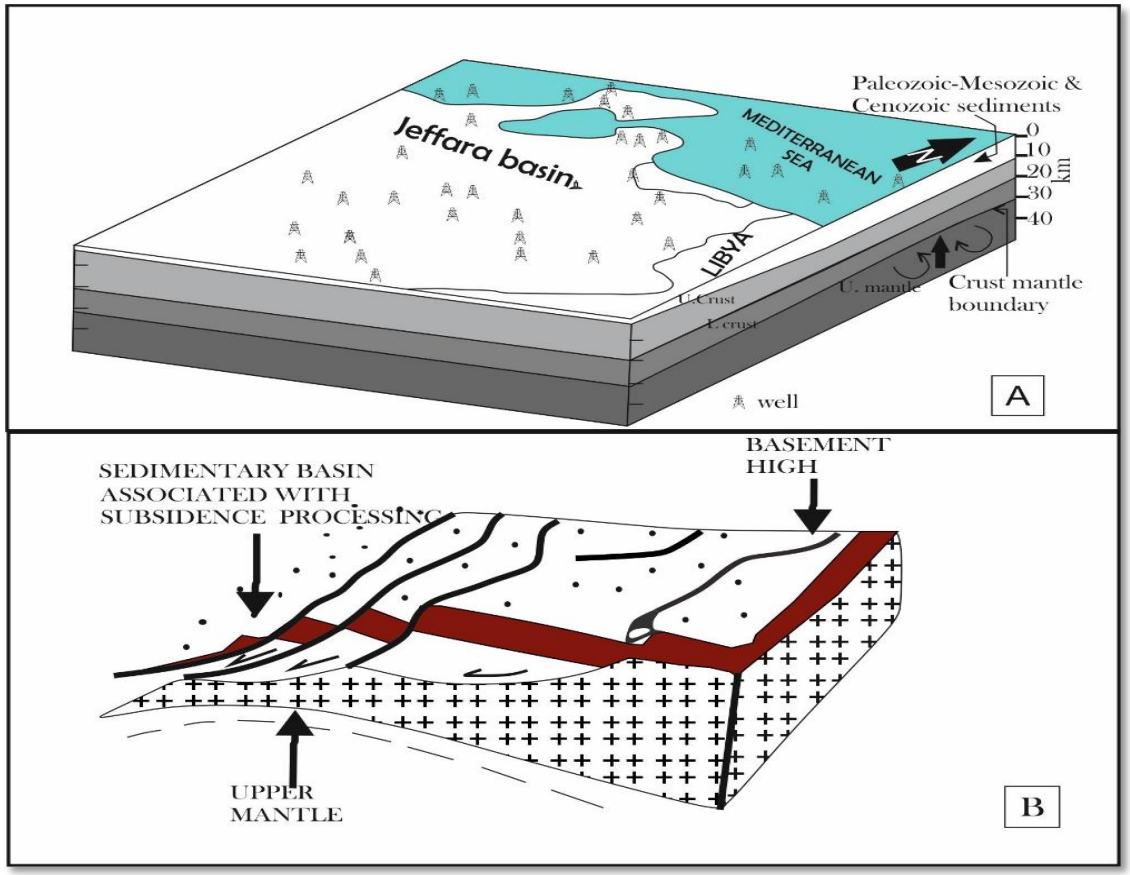
Paleozoic-Mesozoic &
Cenozoic sediments
Jeffara basin
MEDITERRANEAN SEA
LIBYA
0
10
20
30
40
km
U. Crust
L. crust
U. mantle
Crust mantle
boundary
well
A
SEDIMENTARY BASIN
ASSOCIATED WITH
SUBSIDENCE PROCESSING
BASEMENT
HIGH
UPPER
MANTLE
B

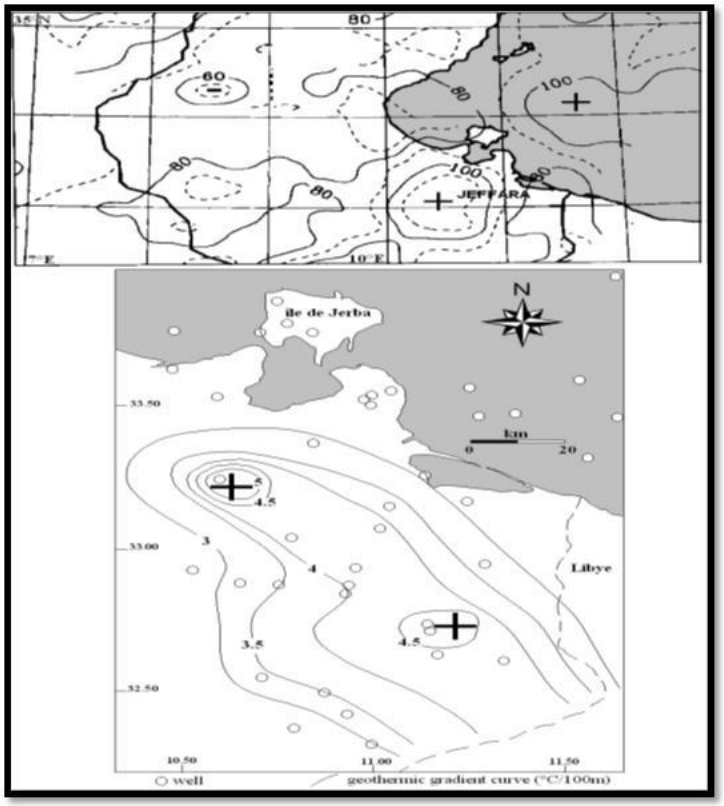
80
60
100
JEFFARA
10°E
Ile de Jerba
N
33.50
33.00
32.50
km
0
20
4.5
3
4
3.5
Libye
10.50
11.00
11.50
well
geothermic gradient curve (°C/100m)

Figure 12

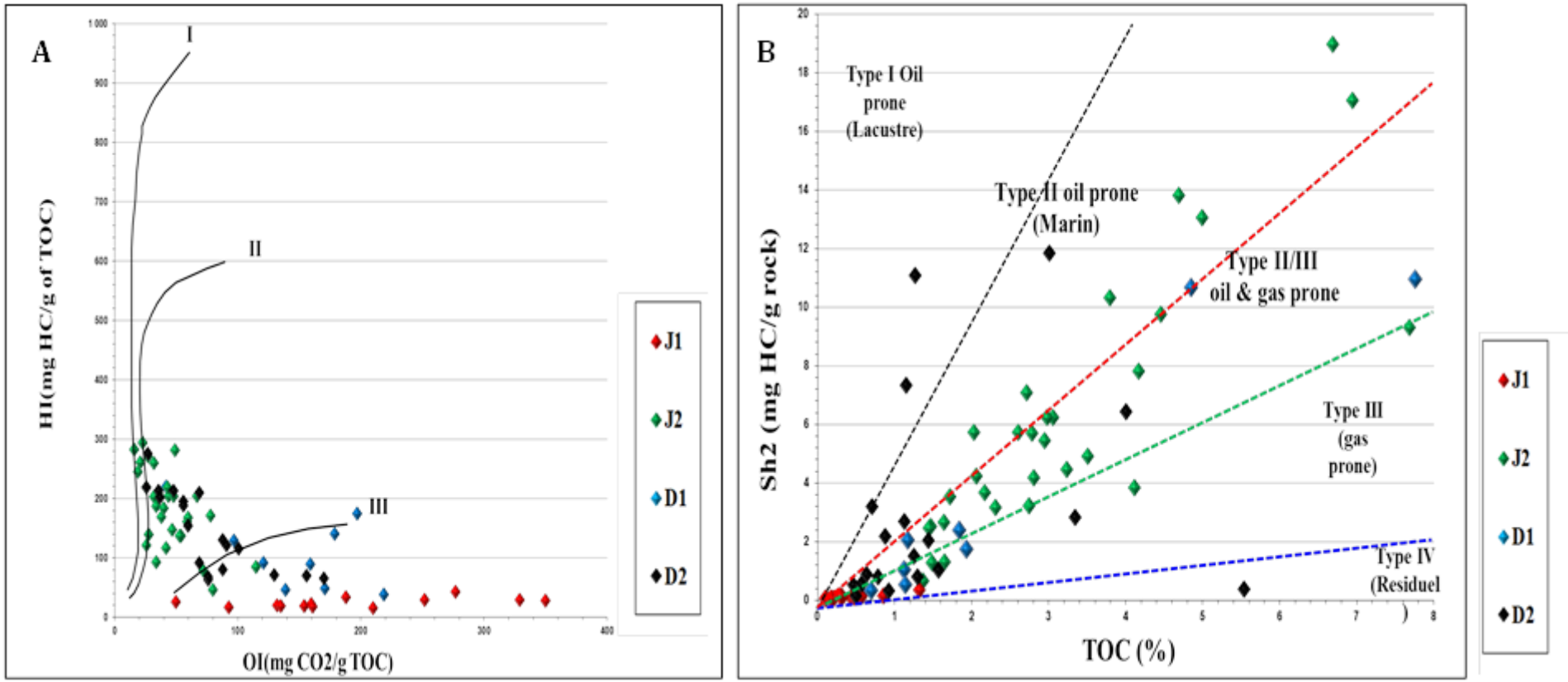
A
I
II
III
HI(mg HC/g of TOC)
OI(mg CO2/g TOC)
J1
J2
D1
D2
B
Type I Oil prone (Lacustre)
Type II oil prone (Marin)
Type II/III oil & gas prone
Type III (gas prone)
Type IV (Residuel)
Sh2 (mg HC/g rock)
TOC (%)
J1
J2
D1
D2

Figure 13

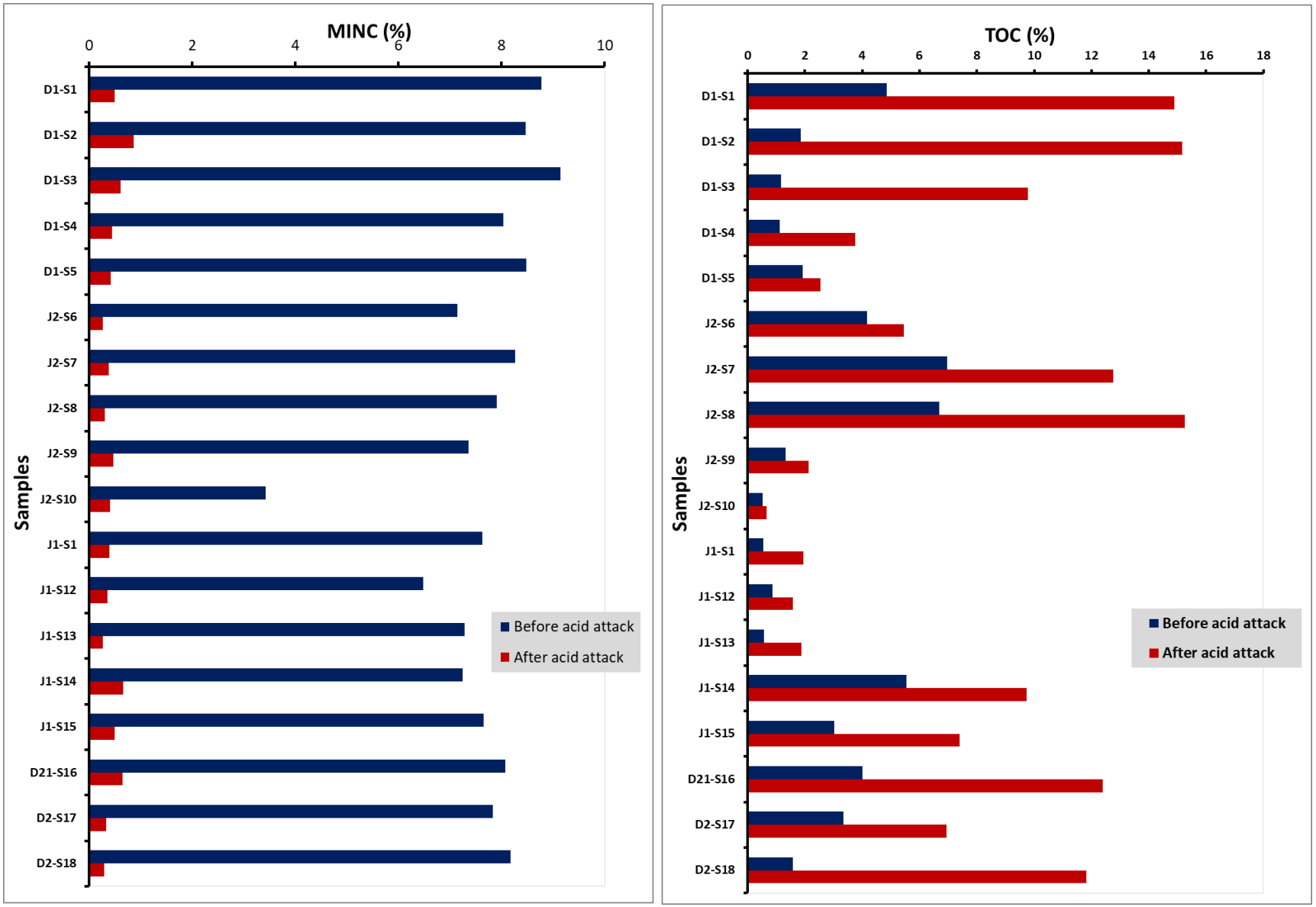
MINC (%)
0
2
4
6
8
10
Samples
D1-S1
D1-S2
D1-S3
D1-S4
D1-S5
J2-S6
J2-S7
J2-S8
J2-S9
J2-S10
J1-S1
J1-S12
J1-S13
J1-S14
J1-S15
D21-S16
D2-S17
D2-S18
Before acid attack
After acid attack
TOC (%)
0
2
4
6
8
10
12
14
16
18
Samples
D1-S1
D1-S2
D1-S3
D1-S4
D1-S5
J2-S6
J2-S7
J2-S8
J2-S9
J2-S10
J1-S1
J1-S12
J1-S13
J1-S14
J1-S15
D21-S16
D2-S17
D2-S18
Before acid attack
After acid attack

Figure 14

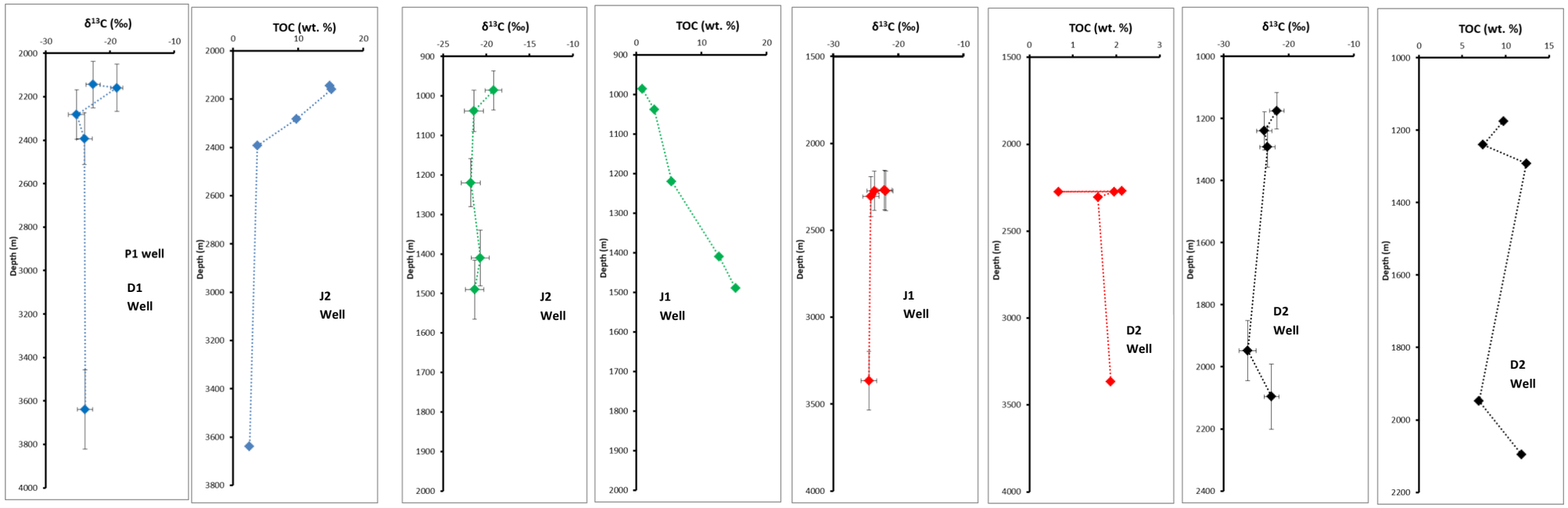

Figure 15

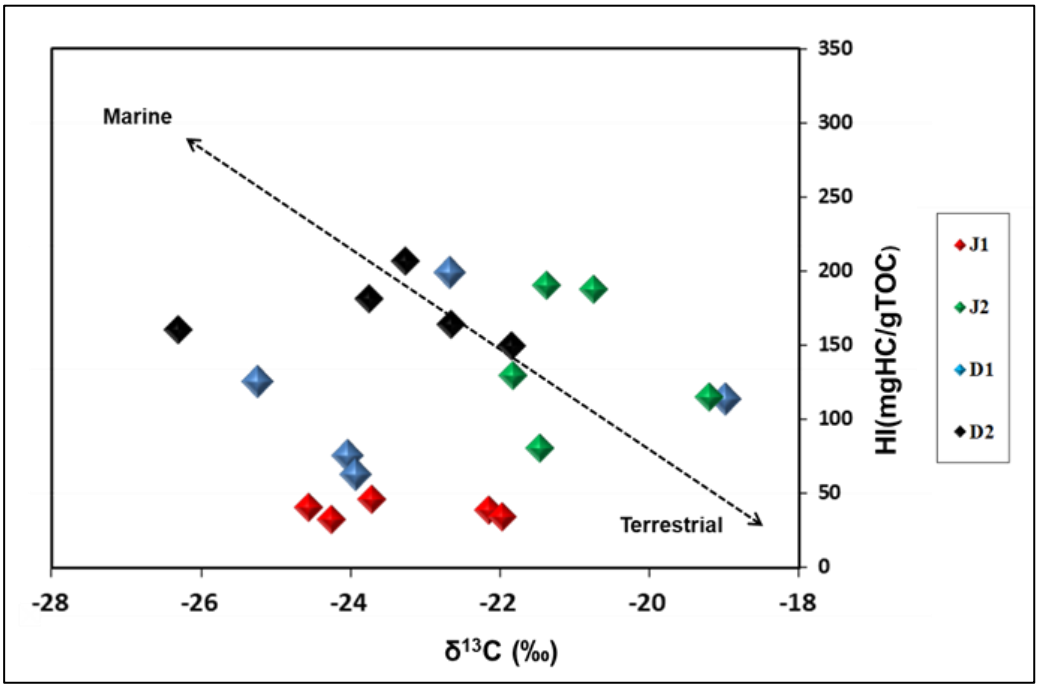

Figure 16

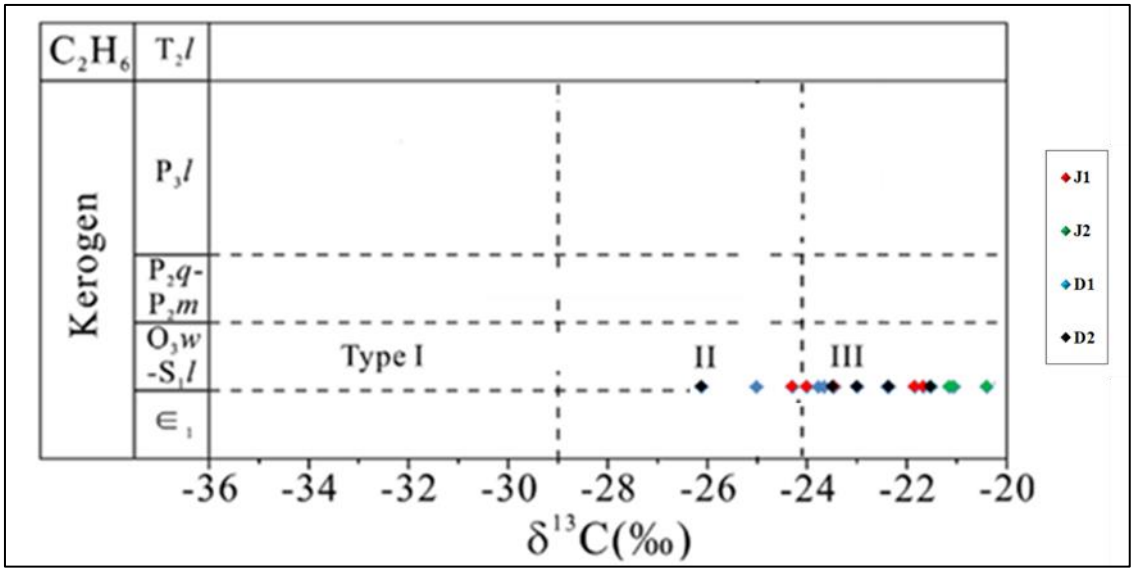

Figure 17

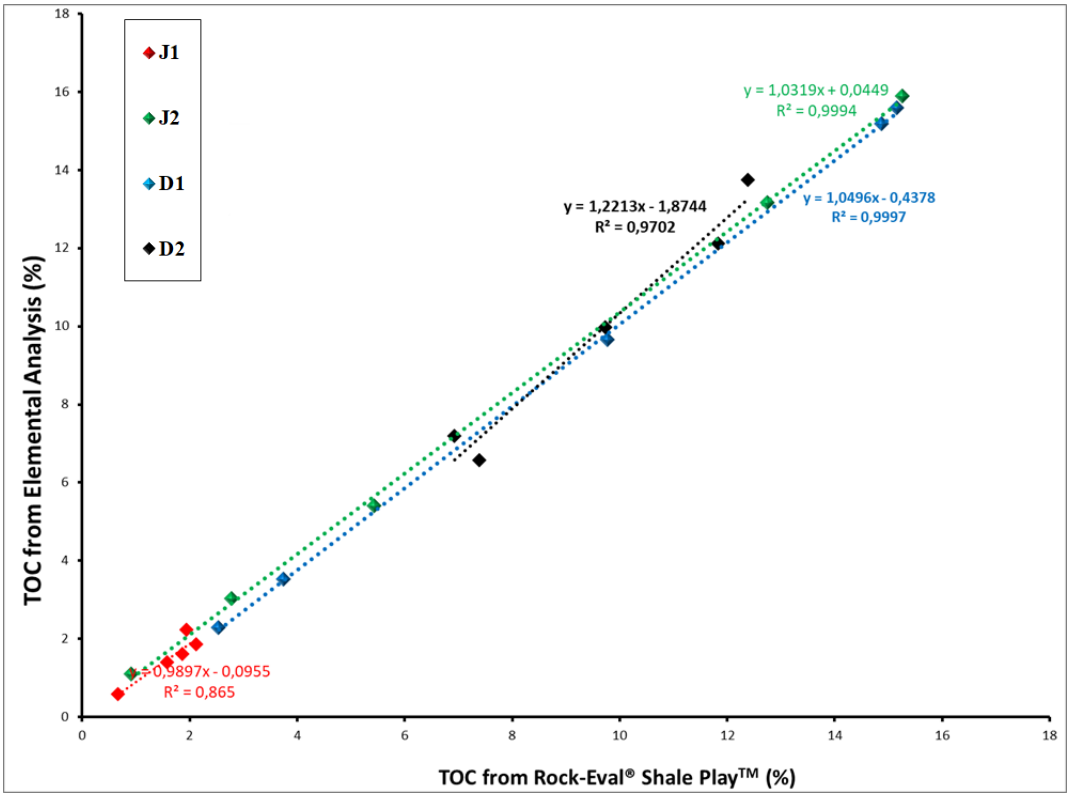

Figure 18

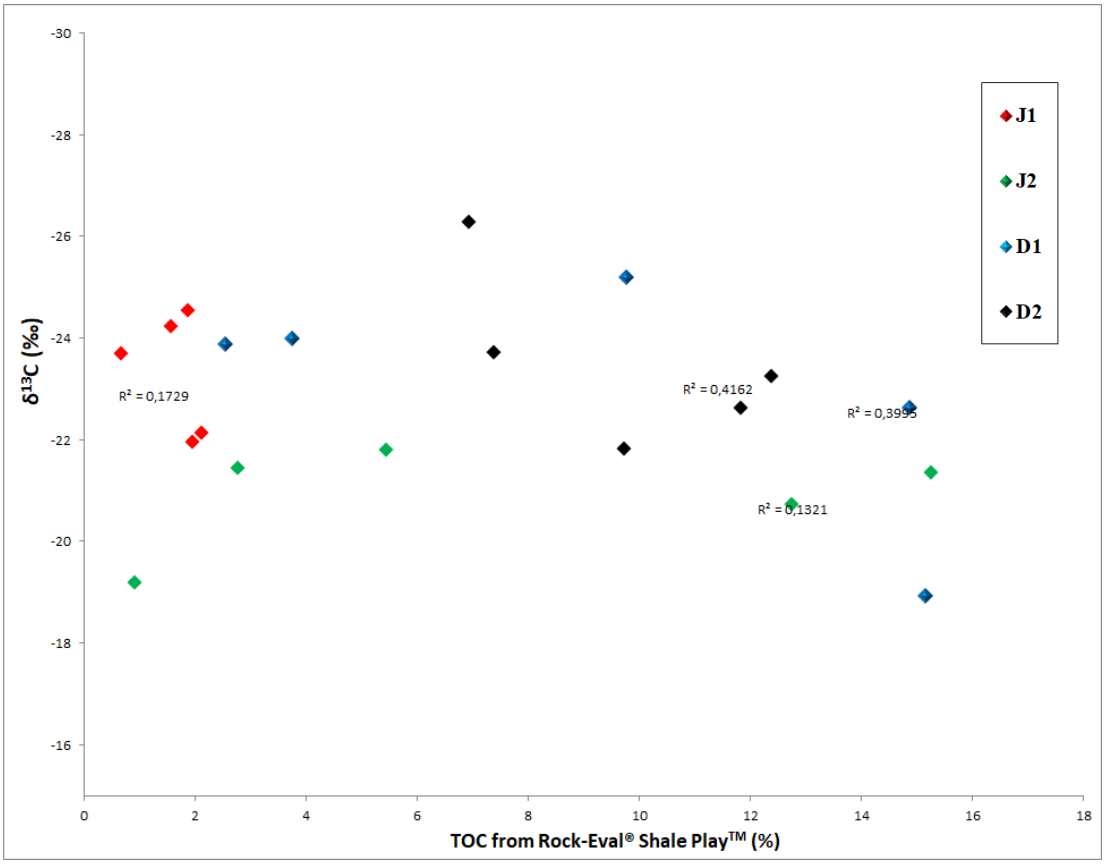

Figure 19

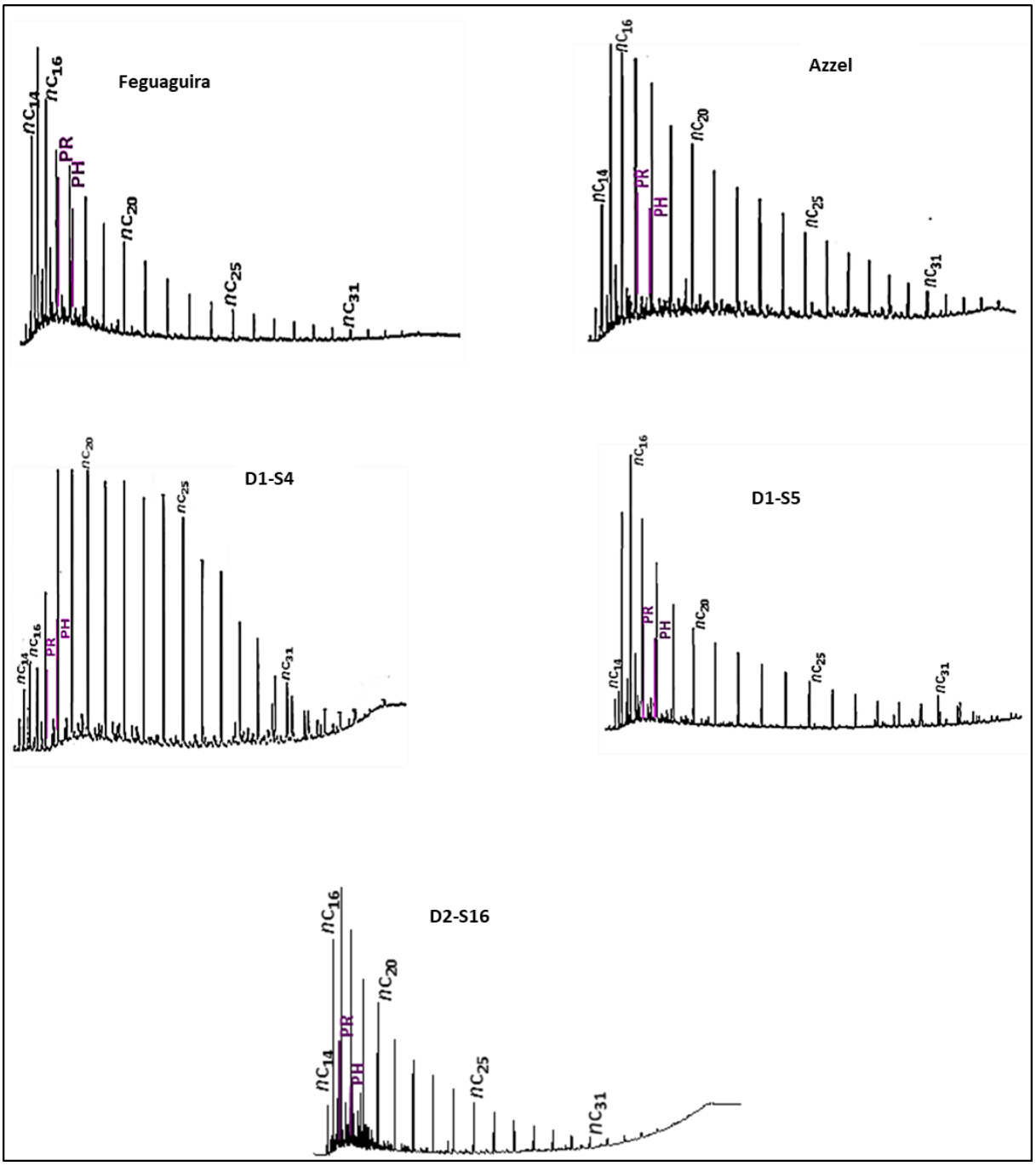
Feguaguira
nC14
nC16
PR
PH
nC20
nC25
nC31
Azzel
nC14
nC16
PR
PH
nC20
nC25
nC31
D1-S4
nC14
nC16
PR
PH
nC20
nC25
nC31
D1-S5
nC14
nC16
PR
PH
nC20
nC25
nC31
D2-S16
nC14
nC16
PR
PH
nC20
nC25
nC31

Figure 20

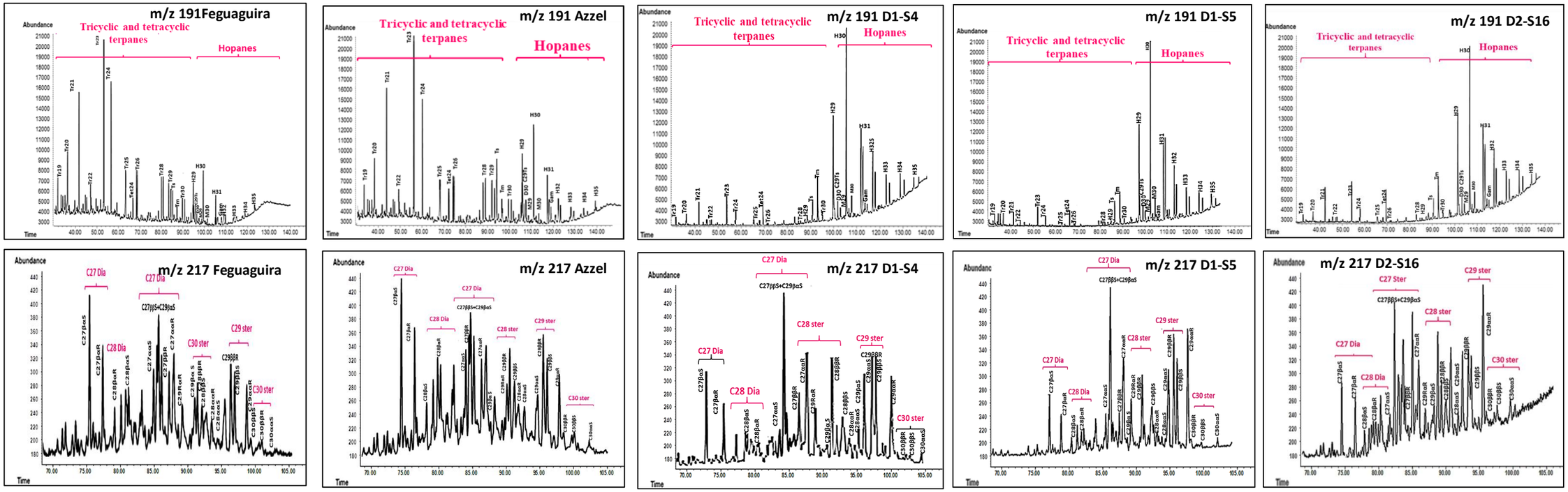
m/z 191Feguaguira
m/z 191 Azzel
m/z 191 D1-S4
m/z 191 D1-S5
m/z 191 D2-S16
Tricyclic and tetracyclic terpanes
Hopanes
m/z 217 Feguaguira
m/z 217 Azzel
m/z 217 D1-S4
m/z 217 D1-S5
m/z 217 D2-S16
C27 Dia
C28 Dia
C30 ster
C29 ster
C28 ster
C27 Ster
Abundance
Time

Figure 21

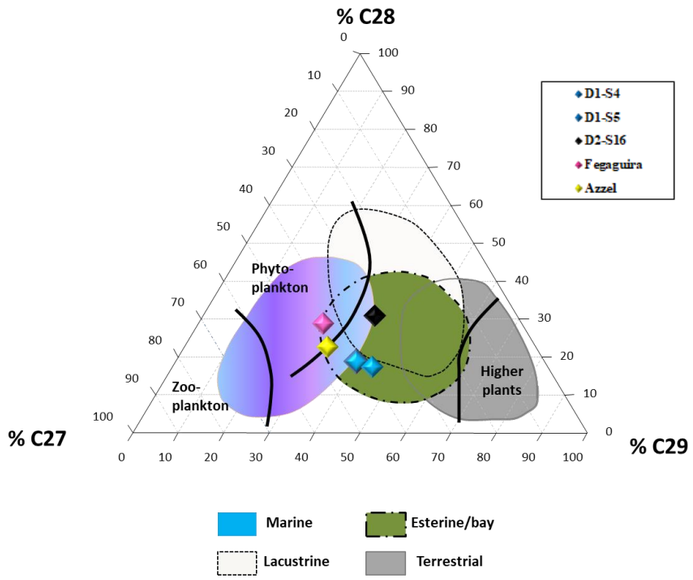

Figure 22

Figure 22

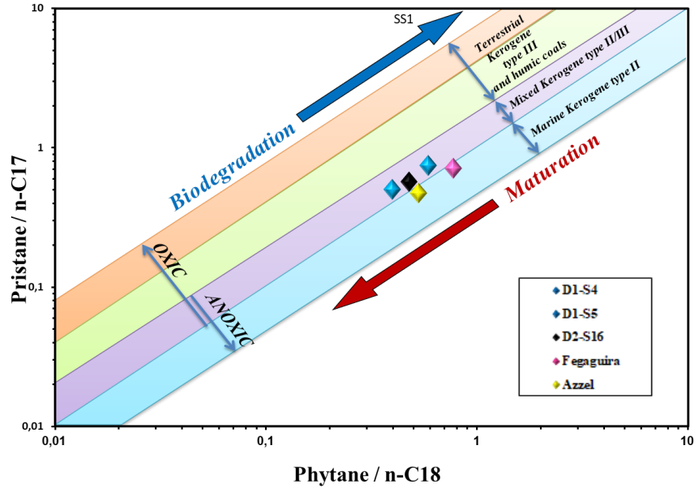

Figure 23

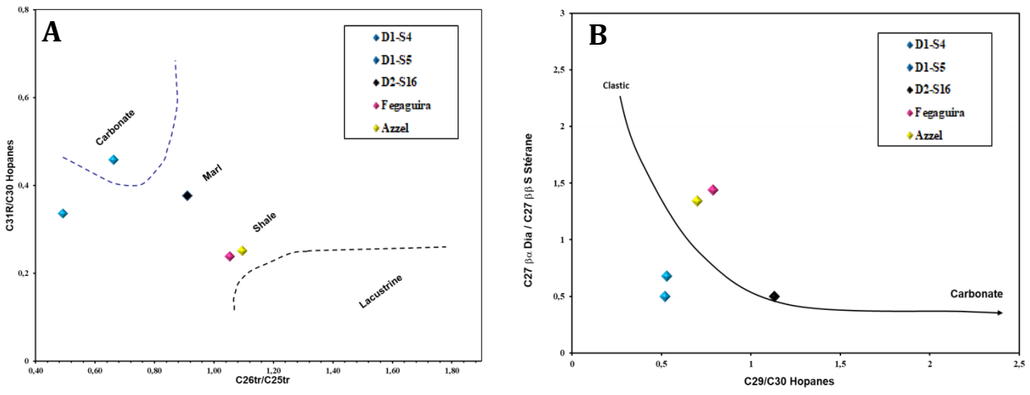

Figure 24

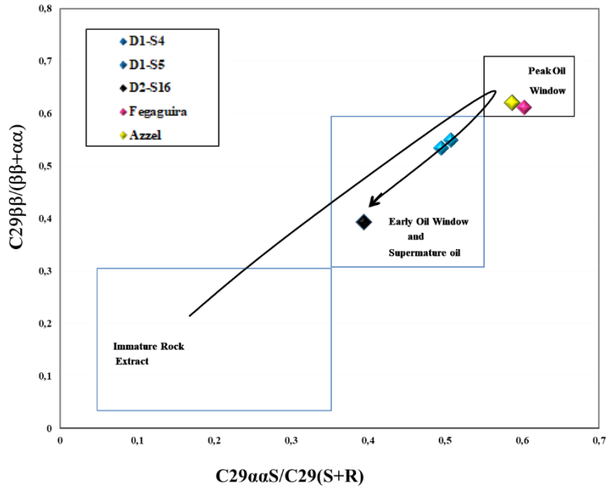

Figure 25